

---

# RAMAN SPECTROSCOPY

Application eBook

# CONTENTS

## Semiconductors

### Evaluation of SiC semiconductors ..... 4

- Evaluation of polymorphism in SiC
- Distribution analysis of 3C-SiC on 4H-SiC wafer
- Evaluating carrier density in SiC
- Non-destructive depth profile measurement of 4H-SiC epitaxial layer
- Evaluation of component in a multi-layer structure of SiC wafer using DSF and MCR analysis

*Tips: DSF (Dual Spatial Filtration)*

### Evaluation of residual stress/strain in a silicon semiconductor ..... 8

- Wavenumber reproducibility in the Si peak
- Stress/strain distribution near interface between nitride film and Si substrate

*Tips: Simultaneous measurement with a Ne lamp*

### Measurement of physical properties of a semiconductor material using photoluminescence ..... 10

- PL measurement of InGaN
- Combined PL/Raman analysis of SiC
- Combined PL/Raman analysis of MoS<sub>2</sub>

*Tips: Laser adjustment and optimization*

*Tips: Automatic grating switching mechanism*

## Material Science

### Evaluating the materials in rechargeable batteries ..... 13

- Evaluation of the cathode
  - Tips: Atmospheric shielding cell and electrochemistry cell*
- Evaluation of the binder
- Evaluation of the anode

### Evaluation of multi-layer ceramic capacitors ..... 15

- Structural phase transition of BaTiO<sub>3</sub> powder by heating/cooling
  - Tips: Heating/cooling stage*
- Evaluating the deterioration of an MLCC using an acceleration test

### Evaluation of carbon materials ..... 17

- Raman imaging of graphene
- Evaluation of carbon nanotubes in the low wavenumber region
- Excitation wavelength dependence of carbon nanotubes
- Analysis of DLC coating distribution of a blade edge
- Raman measurement of DLC coating on plastic bottles

### Evaluation of inorganic materials ..... 21

- Detection of differences in crystal structure in inorganic materials
- Analysis of surface iron oxidation states
  - Tips: SSI (Surface Scan Imaging)*



## Polymers

Evaluation of the physical properties of polymers .....	24
Visualization of sea-island structure of a polymer blend	
Evaluation of crystallization in a micro area on a plastic bottle	
Non-destructive depth profile measurement and MCR analysis of polymer laminate	
Evaluation of the orientation of polyethylene by Raman spectroscopy	

## Biotechnology

Analysis of the orientation and secondary structure of spider silk.....	27
<i>Tips: Polarization measurement using IQ Frame</i>	

## Environmental Science

Analysis of microplastics .....	30
Analysis of AMPs	
Combined IR/Raman analysis of plastic particles	
<i>Tips: Combined analysis by IQ Frame</i>	
<i>Tips: JASCO Particle Analysis</i>	

## Pharmaceuticals

Evaluating the distribution of components in pharmaceutical tablets .....	35
Component distribution in a pharmaceutical tablet	
<i>Tips: Analysis Wizard</i>	

Evaluating the crystal polymorphs in pharmaceutical development .....	37
---	----

- Measurement of trehalose polymorph
- Measurement of indomethacin polymorph
- Measurement of carbamazepine polymorph
- Temperature stability evaluation of pharmaceutical drug
- Tips: Low wavenumber measurement*

## Art Science

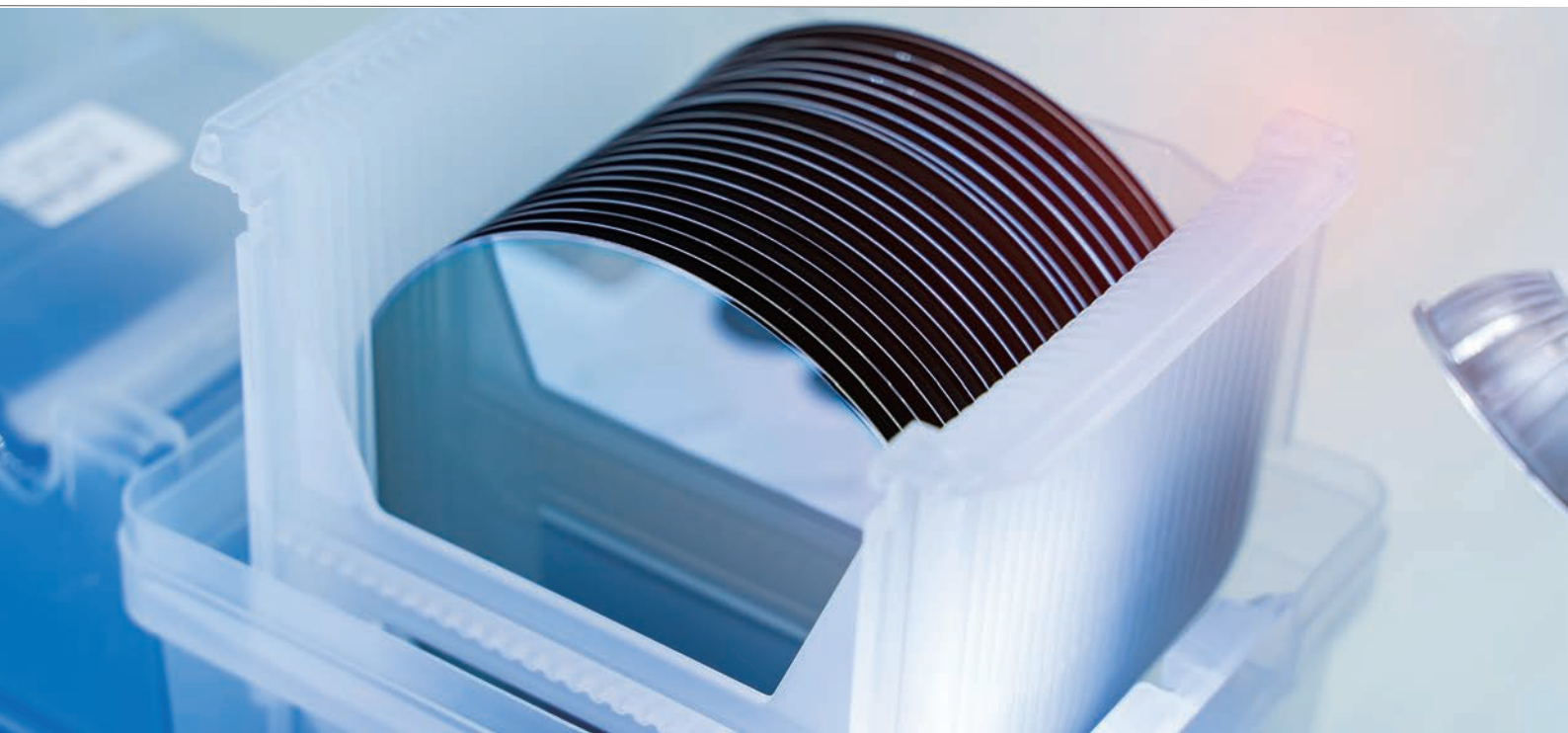
Non-destructive analysis of artworks and other cultural assets .....	40
Qualitative analysis of colorants	
Combined analysis of toner pigment	
Non-destructive analysis of archaeological art	

## Forensic Science

Forensic analysis of vermilion ink .....	43
Measurement using 532 nm laser	
Measurement using 785 nm laser	
Analysis of the results	

Commercial pen ink identification in a handwriting document .....	45
---	----

- Raman spectra of each pen
- Determining the stroke order of intersections using Raman spectroscopy
- Tips: Spectral search program - KnowItAll -*



## Evaluation of SiC Semiconductors

Recently, silicon carbide (SiC) has been attracting attention in the field of power devices that can convert and control electric power. Compared with silicon (Si), it has good performance including low on-resistance, high-speed switching and good thermal stability. Since it can be used in the manufacture of miniaturized power devices with low power consumption, it is expected to have a huge impact on energy saving and CO<sub>2</sub> emissions. In addition, since it has the superior features of high breakdown voltage and high temperature operation, it can be used under severe environmental conditions that can be challenging for Si-based semiconductors.

SiC semiconductors can be used where high voltage and temperature are considered important in a variety of fields that require high electric power (such as power generation, electric vehicles, railways, etc).

SiC semiconductors are a key factor in achieving carbon neutrality; which has led to an increase in R&D of high quality semiconductor materials.

Raman spectroscopy is often used for investigating fundamental chemical composition, orientation, crystallization, density, stress and temperature of semiconductor materials. It can also be used for various structure-property evaluations such as impurities, defects in the semiconductor materials and composition ratio of mixed crystal semiconductors. Raman spectroscopy has also been utilized for estimating carrier density of group III-V semiconductors.

Wafers with dimensions up to 8 inch can be measured using a large sample compartment making it possible to evaluate full-sized samples without damage (Fig. 1).

This section shows the evaluation examples of SiC by Raman spectroscopy.

1) NEDO, *TSC foresight* vol. 103, <https://www.nedo.go.jp/content/100939129.pdf> (2021).



Fig. 1 Large sample compartment for 4/6/8 inch wafer.

## Evaluation of Polymorphism in SiC

It is well known that SiC crystal structure has more than 200 different polymorphs depending on the atomic arrangement; each of these has different physical properties. Among these many polymorphs, the most valuable start from 4H, which has the largest band gap and high mobility. One current hot topic and a significant challenge has been to selectively grow these crystals. Raman spectroscopy is a proven tool used to evaluate and determine polymorph type by analysis of peak patterns due to lattice vibrations in the crystal structure; these appear in the low wavenumber region where measurement is more difficult when using IR spectroscopy.

This section shows the results of Raman measurement of two different SiC monocrystals with 0.33 mm thickness prepared by vacuum sublimation under various conditions (Fig. 2). By comparing the measured spectra in the range of 150–200  $\text{cm}^{-1}$  and 700–800  $\text{cm}^{-1}$  with reference spectra in a published paper<sup>2)</sup>, the two samples were determined to be 6H and 4H polymorphs, respectively.

2) Nakashima, S. & Harima, H., *Phys. Stat. Sol. (a)* **162**, 39 (1997).

(Raman application data: 220-AN-0008)

We would like to express our sincere gratitude to Prof. Inushima and Mr. Ohta of Course of Electrical and Electronic System in Tokai University, Japan, for providing the samples in this evaluation.

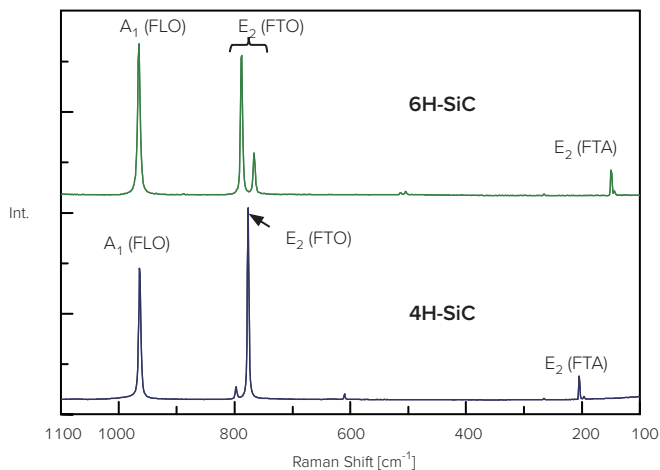


Fig. 2 Raman spectra of 6H-SiC and 4H-SiC polymorphs (532 nm excitation)

### Distribution Analysis of 3C-SiC on 4H-SiC Wafer

Raman imaging measurement can detect the location of polymorphs, which differ from the wafer substrate. In order to verify its usability, Raman imaging measurement of 3C-SiC defects in a 4H-SiC wafer was performed (Figs. 3, 4 and 5). Distribution information of the defects could be obtained clearly by creating a chemical image of the specified bands.

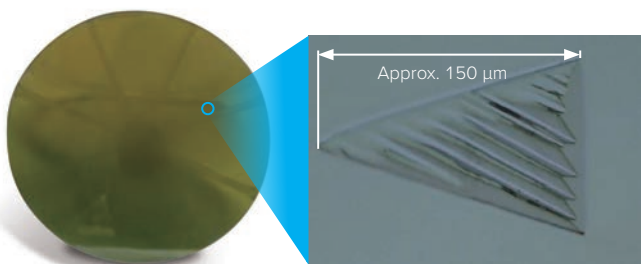


Fig. 3 Observation views of 4H-SiC wafer sample and defect in the wafer.

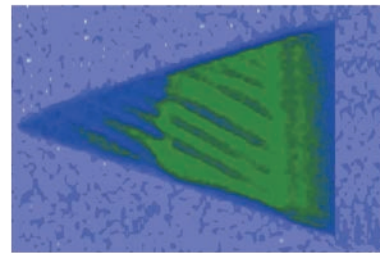


Fig. 4 Raman imaging measurement result. (green: TO peak intensity of 3C-SiC, blue: FTO peak intensity of 4H-SiC)

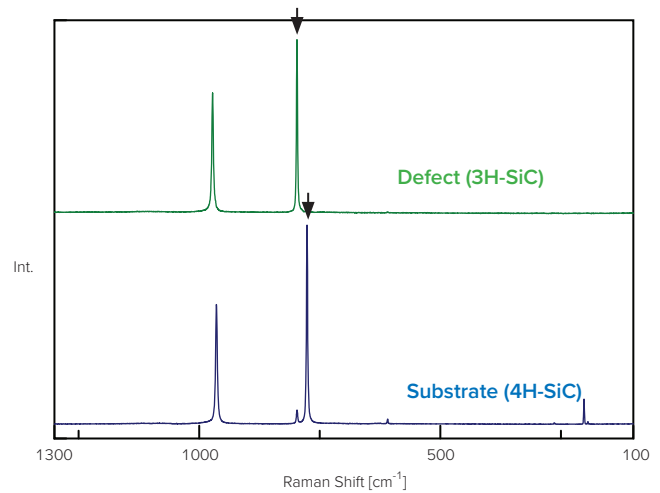


Fig. 5 Raman spectra of each part.

Furthermore, Raman spectroscopy can provide depth profile information in addition to surface analysis.

As an example, a depth profile measurement of a 3C-SiC defect was performed (Fig. 6). 3C-SiC was distributed in the depth direction as well as at the surface.

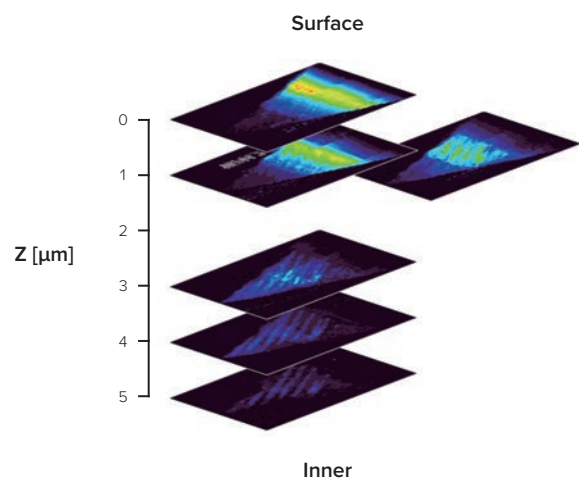


Fig. 6 Stack view of defect part (3C-SiC).

### Evaluating carrier density in SiC

In the manufacturing process of semiconductor materials, it is not unusual to dope the pure semiconductor with an impurity to increase the density of free electrons and electron holes as the carrier. Raman spectroscopy is a simple method to estimate the carrier density in n-type semiconductors.

In polar semiconductors (such as GaN, GaAs and SiC), longitudinal waves and transverse waves due to lattice vibration in the crystal can be observed separately in a Raman spectrum. Collective oscillation of free electrons that exist in n-type semiconductors as the carrier is called a plasmon, which is a longitudinal wave similar to a sound wave. This oscillation is the same type of wave as the longitudinal wave due to lattice vibration, longitudinal optical (LO) phonon and therefore they interact with each other. This interaction becomes greater with increasing carrier density and this relevancy makes the peak position of the longitudinal wave due to lattice vibration shift to a higher wavenumber. Such peak shifts are named as  $L_+$  and  $L_-$ . In the evaluation of SiC, only the  $L_+$  peak can be observed using Raman spectroscopy. It is well known that this peak shifts to higher wavenumbers with broadening peak shape when the carrier density increases, and accordingly, the absolute carrier density can be evaluated from the peak position.

This section shows the results of Raman measurement of 3 types of 4H-SiC monocrystal grown to 0.33 mm thickness using several different conditioned sublimation methods (Fig. 7).

As the carrier density increased, the peak shape became broader and the peak shifted to higher wavenumbers.

(Raman application data: 220-AN-0008)

We would like to express our sincere gratitude to Prof. Inushima and Mr. Ohta of Course of Electrical and Electronic System in Tokai University, Japan, for providing the samples in this evaluation.

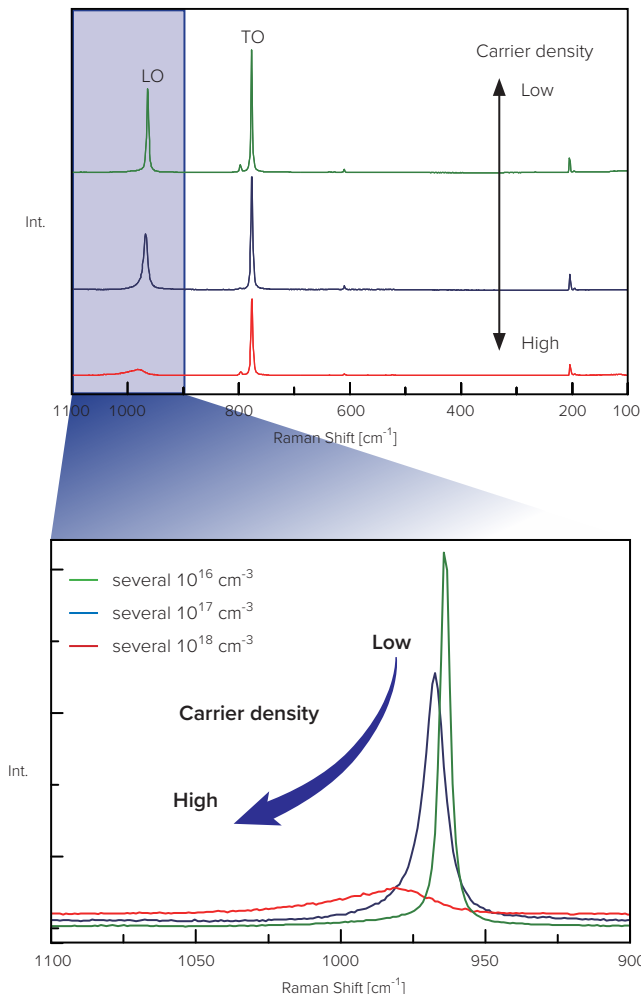


Fig. 7 Change of Raman spectrum of 4H-SiC due to carrier density. (532 nm excitation)

## Non-Destructive Depth Profile Measurement of 4H-SiC Epitaxial Layer

Raman spectroscopy can provide depth profile information without destroying the sample.

In this example, a depth profile measurement of a 4H-SiC wafer was performed (Fig. 8). 30 spectra were obtained at 0.5  $\mu\text{m}$  intervals from a focal point at the surface on the wafer. It was confirmed that the longitudinal optical (LO) peak of 4H-SiC (950 to 1000  $\text{cm}^{-1}$ ) changed depending on the depth. This demonstrates that the epitaxial layer with low carrier density was on the surface and the high carrier density was in the inner layers. It should be noted that the epitaxial layers with high/low carrier density could be clearly observed using JASCO's unique confocal optical system - Dual Spatial Filtration (DSF: refer to page 7). It is considered that the Z distance (moving distance of the stage) multiplied by the refractive index of the SiC is the actual depth.

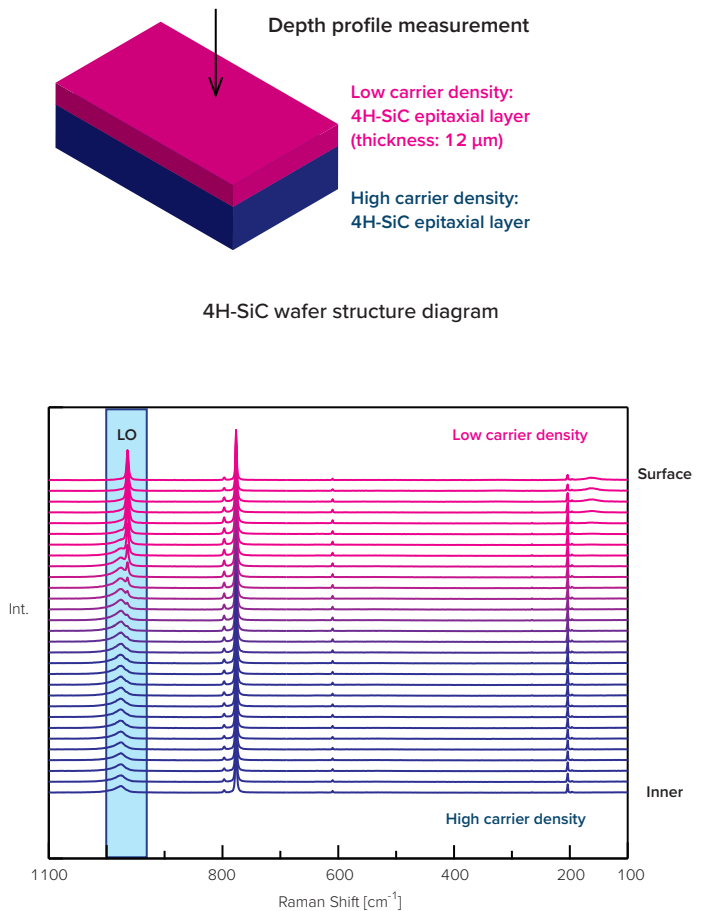


Fig. 8 Non-destructive depth profile measurement of 4H-SiC wafer.

## Evaluation of Components in a Multi-Layer SiC Wafer

It is often difficult to perform depth profile measurement of samples with multiple or thin epitaxial layers by Raman spectroscopy because the spectra may become mixed. Dual Spatial Filtration (DSF) offers significantly higher spatial resolution measurement. Also, multivariate curve resolution (MCR) analysis can easily deconvolve each component spectrum, so that the carrier densities of each layer can be evaluated (Fig. 9).

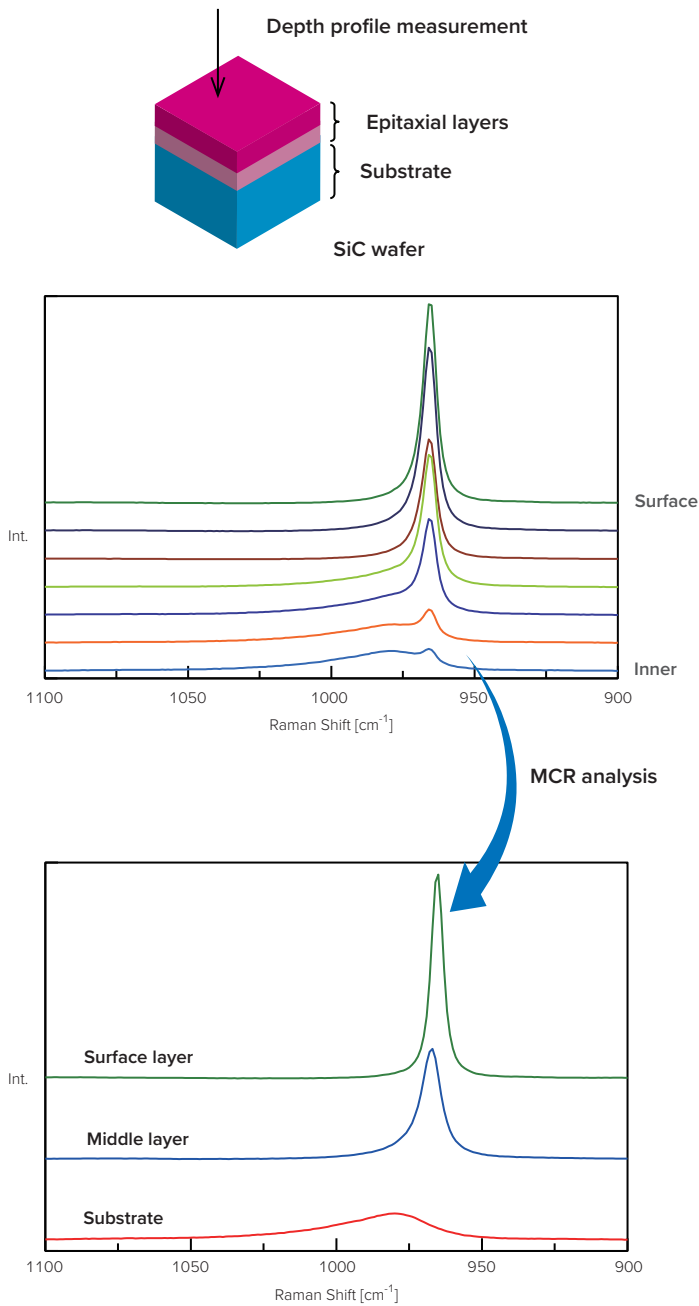


Fig. 9 Non-destructive depth profile measurement of SiC wafer.

The Intensity profile of a spectrum can provide visual information about epitaxial layer location<sup>3)</sup>. In addition, since the carrier density quantified by secondary ion mass spectrometry (SIMS) measurement is correlated with longitudinal optical (LO) peak shift, it is possible to estimate the carrier densities of each layer using principal component spectra<sup>3)</sup>.

3) Tawara, T., Ryo, M. & Miyazato, M., *Fuji Denki Gihō* vol. 90 no.4, 214-218 (2017).

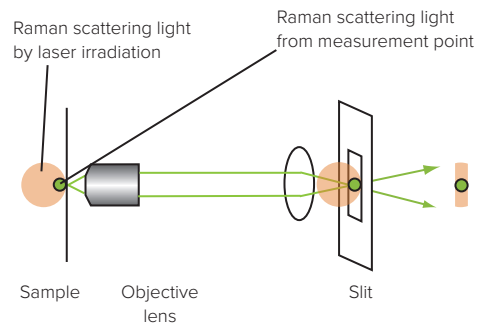
## Tips

### DSF

#### (Dual Spatial Filtration)

DSF is the mechanism that consists of a confocal aperture and pinhole slit, and offers improved depth resolution (1  $\mu\text{m}$  at Si substrate). Improvement of depth resolution makes it possible to acquire a Raman scatter spectrum at the exact measurement point (focal plane) only (Fig. 10).

#### <Slit confocal optics>



#### <DSF confocal optics>

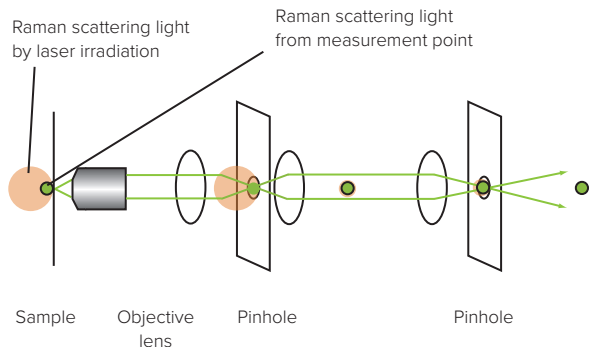


Fig. 10 Principle of DSF.



## Evaluation of Residual Stress/Strain in a Silicon Semiconductor

As the dimensions of semiconductor devices continue to shrink, there is an increased risk of cracking due to extremely localized stress and strain. It is therefore important to have an effective means of evaluating the stress/strain in this type of material. Raman spectroscopy is a powerful tool for investigating the distribution of stress/strain at high spatial resolution in different regions of a target sample.

Peak shift in a Raman spectrum is a useful reference for determining the extent of stress/strain in a crystalline material. Applied stress decreases the lattice constant, with the peak position shifting to higher wavenumbers. Conversely, strain shifts the peaks to lower wavenumbers (Fig. 1).

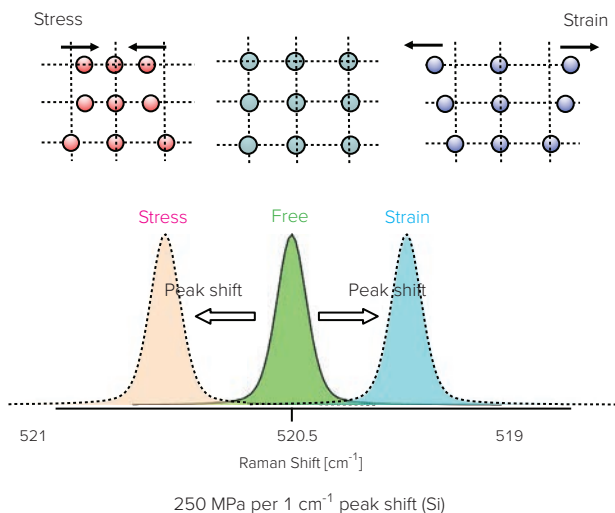


Fig. 1 Stress/strain evaluation of Si.

In the case of crystalline silicon (Si), a peak shift of  $1\text{ cm}^{-1}$  corresponds to a pressure of  $250\text{ MPa}$ <sup>1)</sup>, and the stress/strain can be evaluated by comparison with free crystalline Si as a reference.

This section shows the evaluation of residual stress/strain in a Si semiconductor by Raman spectroscopy.

1) Anastassakis, E., Pinczuk, A., Burstein E., Pollak, F. H. & Cardona M., *Solid State Commun.* **8**, 133 (1970).

### Wavenumber Reproducibility in the Si Peak

Since the shifts in silicon peak position are sensitive to changes in environmental temperature and overall optical system rigidity, the stability of the entire Raman microscope is important for evaluating very slight residual stress/strain. In order to verify the stability of the Raman microscope, a time-course measurement of the silicon peak was performed (Fig. 2). Peak shift of  $0.01\text{ cm}^{-1}$  or less could be detected, and this result demonstrates that this system has high stability.

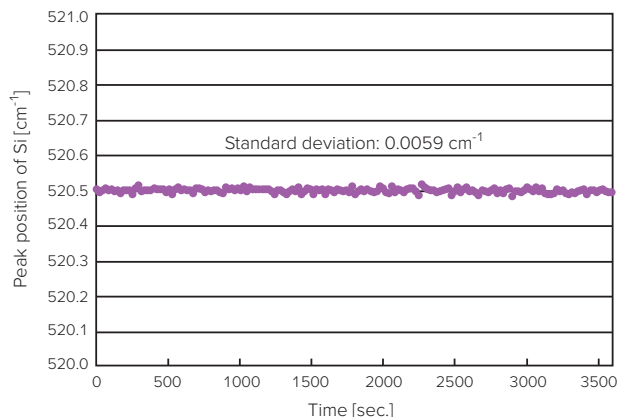


Fig. 2 Si peak position monitoring result.

## Stress/Strain Distribution Near Interface Between Nitride Film and Si Substrate

Since Raman spectroscopy can be used to evaluate the stress/strain in a Si substrate, it is also possible to observe the distribution of stress/strain using Raman imaging measurement. An approximately 60  $\mu\text{m}$  square region at the interface between a Si substrate and a nitride film was evaluated using Raman imaging measurement to determine the stress/strain distribution within the substrate (Figs. 3, 4 and 5). Chemical imaging of the Si-peak position revealed that the stress/strain was generated in the nitride film and Si, respectively. These results indicate that Raman microscopy is an effective tool for evaluating the distribution of stress/strain at micron scale.

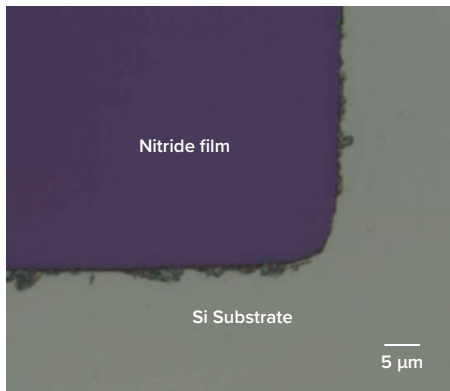


Fig. 3 Observation view.

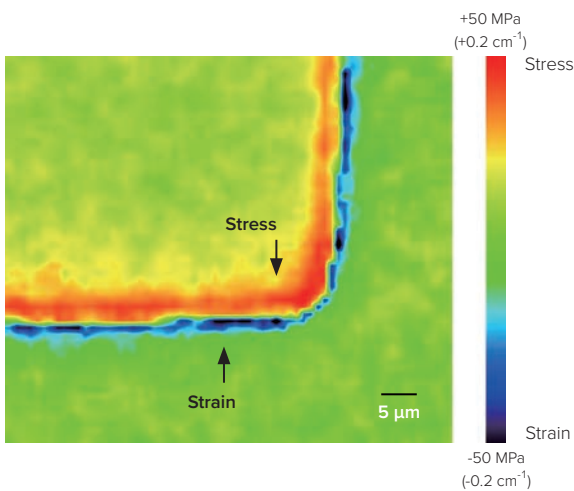


Fig. 4 Raman imaging measurement result.  
(Si peak position)

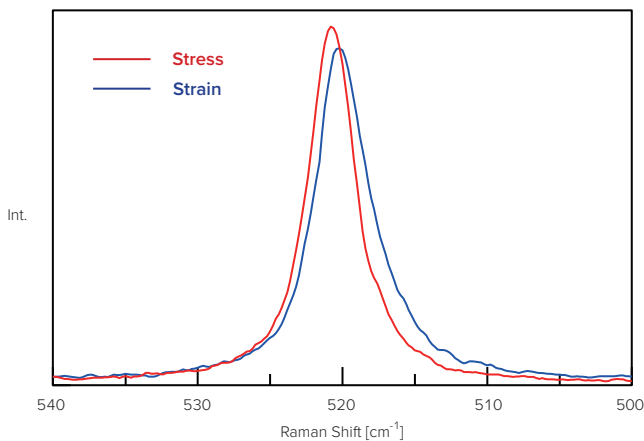


Fig. 5 Raman spectra of each point.

## Tips

### Simultaneous Measurement with a Ne Lamp

The NRS series of Raman microscopes include a Ne lamp (as standard) for absolute wavenumber correction. Monitoring the Ne peak position allows accurate discrimination of shift caused by temperature and/or stress/strain in a sample. By measuring a Raman spectrum and Ne emission lines simultaneously, it is possible to measure a peak shift extremely accurately (Fig. 6). In the following cases it is recommended that a Ne lamp is used for stress/strain measurement. (1) Long measurement time (2) Thermal drift in the spectrograph affects the stress/strain measurement.

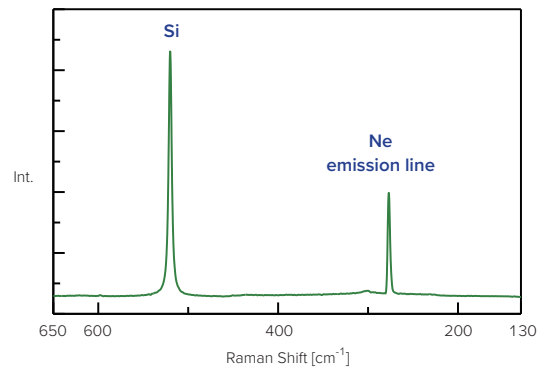


Fig. 6 Simultaneous measurement with the Ne lamp.



# Measurement of the Physical Properties of a Semiconductor Material using Photoluminescence

Emission intensity and wavelength of photoluminescence (PL) can provide a variety of information such as the composition ratio and carrier density in a compound semiconductor. Raman microscopy can perform PL measurement by changing the optical configuration (laser, filter and grating), and can also perform PL and Raman measurement at same measurement position.

This section shows the evaluation of semiconductor materials using PL measurement.

## PL Measurement of InGaN

The band-gap of Indium gallium nitride (InGaN), which is used in the manufacture of LEDs depends on the indium ratio. However, increasing the amount of indium makes it difficult to grow uniform crystals and the composition of the crystal tends to be irregular.

PL measurement can be used to observe the specific peaks of InGaN/GaN (Fig. 1), making it possible to evaluate its lack of composition uniformity.

Since PL measurement can detect the differences in indium composition, the in-plane distribution of the indium composition ratio can be obtained using PL imaging. As an example, PL imaging measurement of InGaN was performed (Fig. 2). The in-plane distribution of the indium composition ratio could be observed with high spatial resolution.

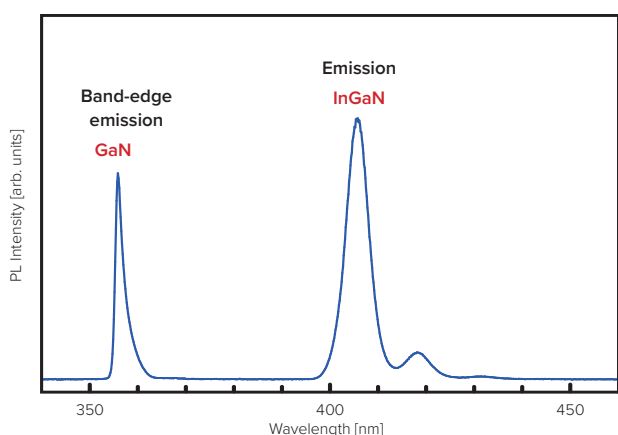


Fig. 1 PL spectrum of InGaN/GaN single quantum well structure.

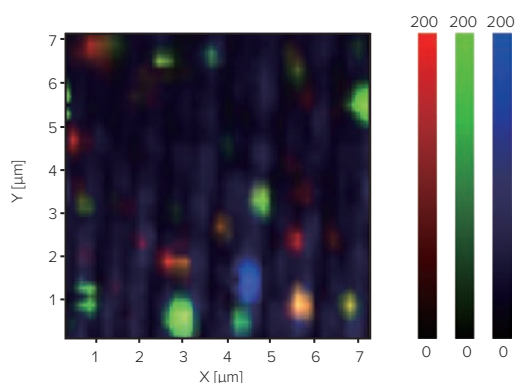


Fig. 2 PL imaging measurement result.  
(red: peak intensity at 437 nm, green: peak intensity at 454 nm, blue: peak intensity at 483 nm)

## Combined PL/Raman Analysis of SiC

PL measurement can be used to evaluate the defect, band-gap and carrier doping in silicon carbide (SiC), and Raman measurement can be used for crystallinity and stress/strain. As an example, PL/Raman imaging measurements of SiC were performed at the same position (Figs. 3, 4 and 5). Emission from defects and impurities could be observed with PL imaging measurement (blue), and the location of different crystal structures could be observed by Raman imaging measurement (red). Combined analysis by PL/Raman measurement provides comprehensive and complementary information.

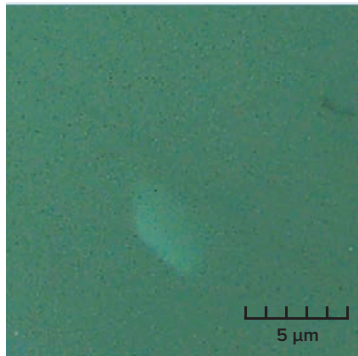


Fig. 3 Observation view.

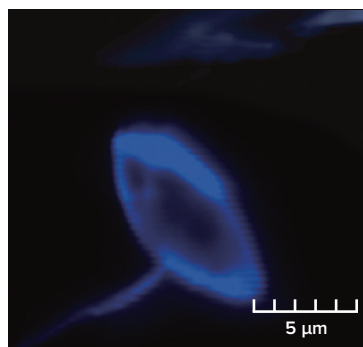


Fig. 4 PL imaging measurement result. (405 nm excitation)

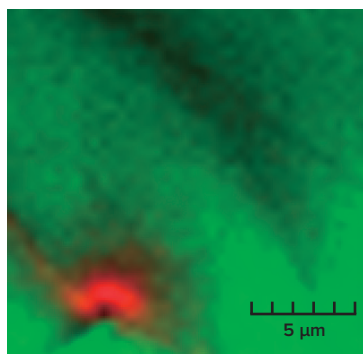


Fig. 5 Raman imaging measurement result. (532 nm excitation)

## Combined PL/Raman Analysis of MoS<sub>2</sub>

Molybdenum disulfide (MoS<sub>2</sub>) has been attracting attention as a 2D material like graphene and is expected to be the material of choice for next-generation transistors. PL measurement can provide band-gap information, which defines the performance of a transistor; this section shows the result of an MoS<sub>2</sub> sample, when the lower half was irradiated with an electron beam.

First, PL imaging of MoS<sub>2</sub> was performed (Figs. 6 and 7). Although no remarkable change could not be found with visible observation, the modulation of band-gap by electron beam exposure could be confirmed from the PL measurements of the areas exposed and unexposed to the radiation.

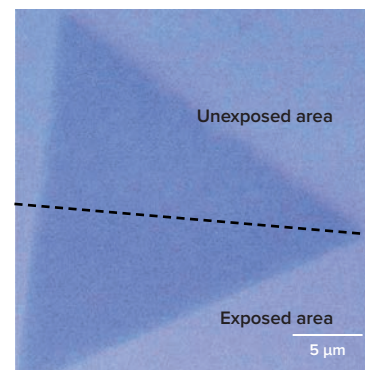


Fig. 6 Observation view.

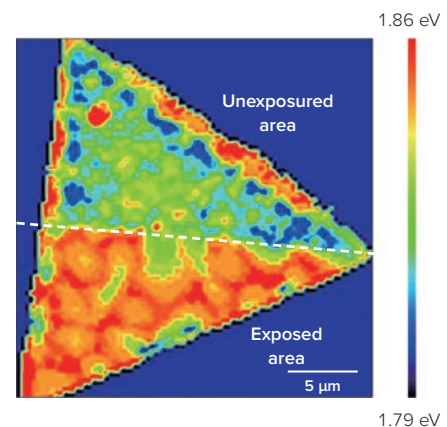


Fig. 7 PL imaging measurement result. (PL peak shift at 670 nm, 532 nm excitation)

Next, Raman imaging measurement of MoS<sub>2</sub> was performed (Fig. 8). A Raman peak shift from stress ( $E_{12g}$ ) could be confirmed from the Raman measurements of the electron beam exposed/unexposed areas. Raman measurement can also obtain information about the number of layers and stress/strain by monitoring the peak shift. Combined analysis with PL/Raman provides comprehensive evaluation of MoS<sub>2</sub>.

We would like to express our sincere gratitude to Prof. Nobuyuki Aoki of Chiba University, Japan, for providing the samples in this evaluation.

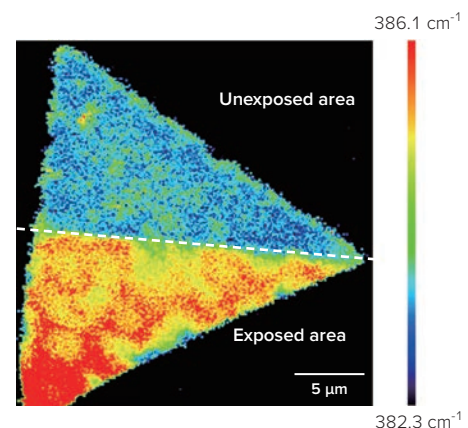
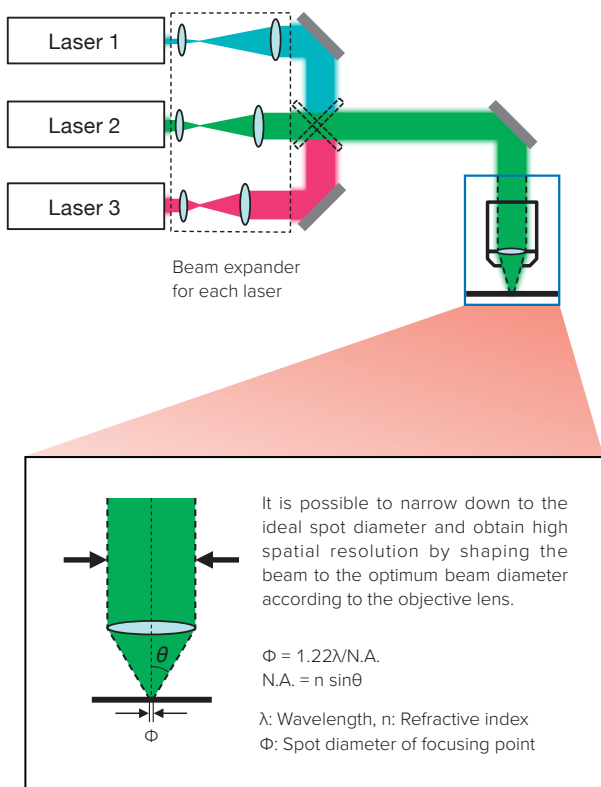


Fig. 8 Raman imaging measurement result. (385 cm<sup>-1</sup> peak shift; E<sub>12g</sub>, 532 nm excitation)

## Tips

### Laser Adjustment and Optimization

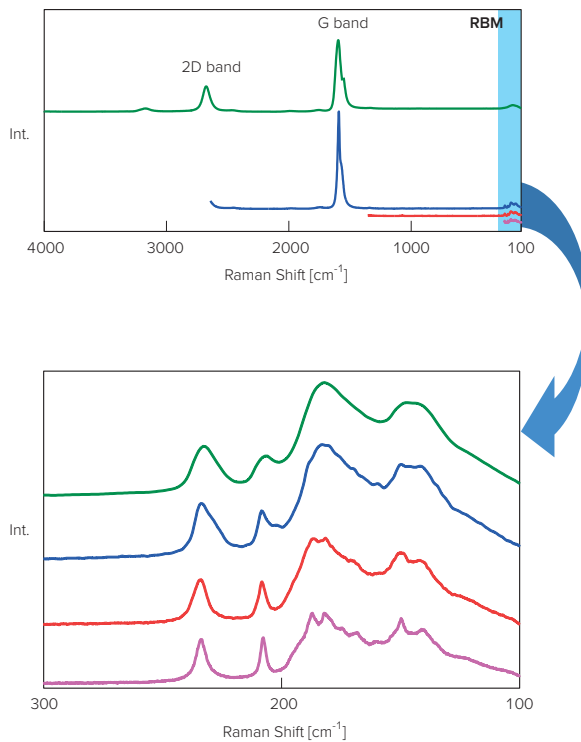
A focusing optical system (beam expander) suitable for each laser is a very useful mechanism for the user. This system is adjusted beforehand so that the optimized light beam is introduced to the objective lens and the high spatial resolution measurement by the ideal focusing is performed. In addition, since the laser switching is performed automatically, it is possible to perform Raman measurement with high reliability without frequent optical adjustment.



## Tips

### Automatic Grating Switching Mechanism

Gratings can be switched automatically through software operation, and it is possible to select a grating suitable for the laser without frequent optical adjustment. By using different gratings, it is possible to acquire Raman spectrum in wide wavenumber region in a single spectrum, and to acquire another with higher spectral resolution in a narrower wavenumber region.



Measurements of carbon nanotube using different gratings  
 (green: 300 L/mm, blue: 600 L/mm,  
 red: 1200 L/mm, pink: 2400 L/mm)

\*RBM (Radial Breathing Mode) : Refer to page 18.



## Evaluating Materials in Rechargeable Batteries

Rechargeable batteries are widely used in daily life. The most common rechargeable battery is the lithium-ion battery, which has become widespread as the power supply for mobile devices. It consists of many materials (such as metal oxides, carbon, polymers and organic solvents) and the quality of these components affect the overall battery performance (Fig. 1).

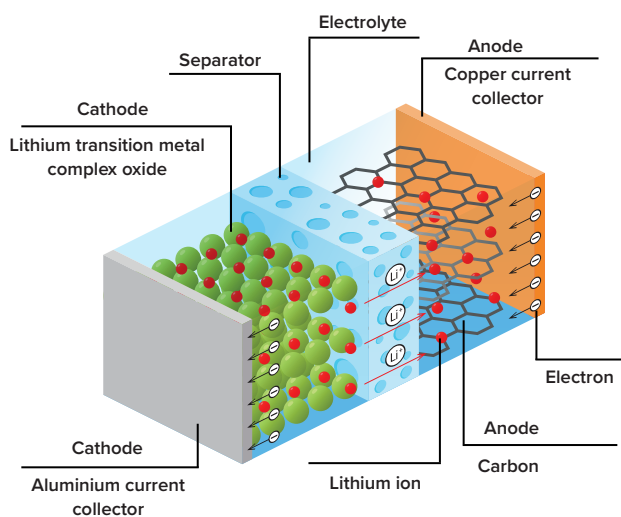


Fig. 1 Lithium ion battery diagram (charge).

In the future, larger batteries will be required for a variety of uses, such as automotive, consumer electronics, energy storage systems, industrial, etc., requiring high reliability as well as high capacity and durability. Therefore, manufacturers are improving quality in existing lithium-ion technology and developing next-generation rechargeable batteries whose performance exceeds the batteries currently being used.

Raman spectroscopy is a powerful tool to evaluate the material quality in rechargeable batteries. It can be used for surface analysis of the anode and cathode, and for deterioration analysis of electrodes by monitoring the differences in crystal structure.

This section shows an example of the analysis of materials found in a rechargeable battery by Raman spectroscopy.

### Evaluation of the Cathode

Transition metal complex oxides (such as  $\text{LiCoO}_2$ ) are used as the cathode of lithium-ion batteries. Raman spectroscopy can be used to measure the spectrum of  $\text{LiCoO}_2$  (Fig. 2) and can be used for deterioration analysis of the product by monitoring the changes.

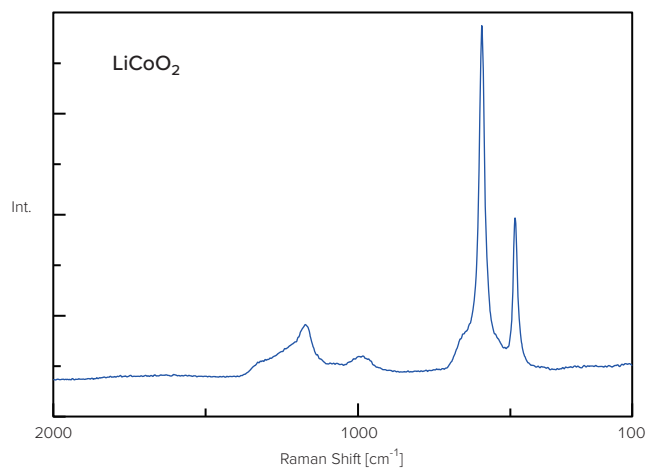


Fig. 2 Raman spectrum of transition metal complex oxide ( $\text{LiCoO}_2$ ).

In addition, information about the size and distribution of active materials can be obtained using Raman imaging<sup>1), 2)</sup>. Raman spectroscopy is also useful for analyzing the battery electrolyte<sup>1), 2)</sup>.

- 1) Celik-Kucuk, A., Yamanaka, T. & Abe T., *Solid State Ionics*, **357**, 115499 (2020).
- 2) Yamanaka T. et al, *ECS Meeting Abstracts*, **MA2020-01**, 203, (2020).

## Tips

### Atmospheric Shielding Cell and Electro-chemistry Cell

Raman spectroscopy is a non-contact, non-destructive technique that can be used to perform analysis that is difficult for other techniques (such as in-situ measurement).

An atmospheric shielding cell can be loaded in a glove-box with an inert gas to seal the sample in an anaerobic environment (Fig. 3). This makes it possible to evaluate sensitive materials such as the electrode material without deterioration or oxidation.

An electro-chemistry cell can be used for monitoring the behavior of an electrode interface during charge/discharge cycles.



Fig. 3 Atmospheric shielding cell.

### Evaluation of the Binder

Polyvinylidene fluoride (PVDF) is a material commonly used as the binder in lithium-ion batteries, and its spectrum can be obtained by Raman spectroscopy (Fig. 4). In addition, distribution information of the active material and binder can be obtained by Raman imaging and is useful for evaluating the lifetime and performance of lithium-ion batteries.

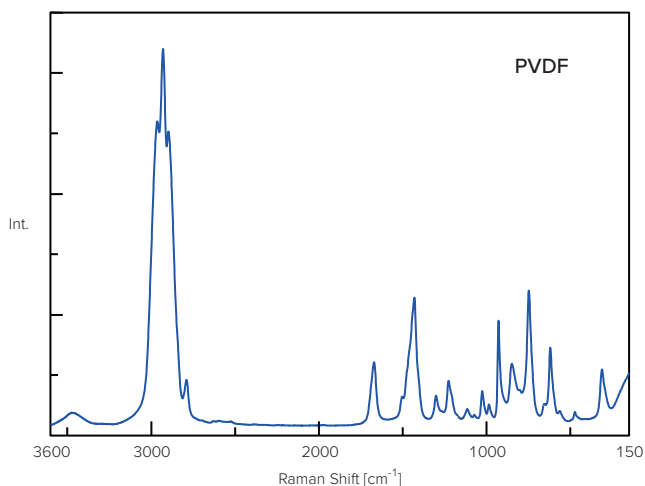


Fig. 4 Raman spectrum of PVDF.

### Evaluation of the Anode

Carbon is mainly used for the anode in lithium-ion batteries. Since Raman spectroscopy can detect structural changes in carbon with great sensitivity it is typically used to perform this material evaluation. Information about quality of graphite can be obtained from the full width at half maximum (FWHM) of the G band (around 1550  $\text{cm}^{-1}$ ) and the intensity ratio between the D band (around 1350  $\text{cm}^{-1}$ ) and G band (Fig. 5).

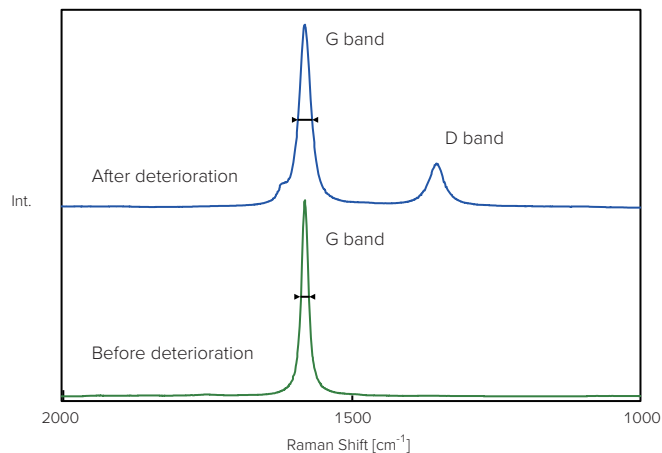


Fig. 5 Raman spectra of graphite.

Raman imaging can be used to check the quality distribution of the carbon material. In this example, Raman imaging of a graphite sample was performed (Figs. 6 and 7). Checking the peak intensity ratio between D and G bands and the FWHM of G band, the distribution of crystallinity and material quality on the electrode surface could be visualized.

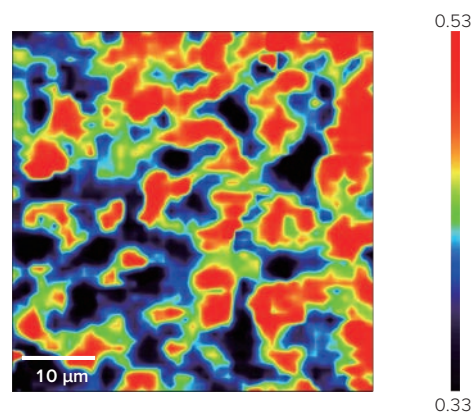


Fig. 6 Raman imaging measurement result. (peak height ratio between G band and D band)

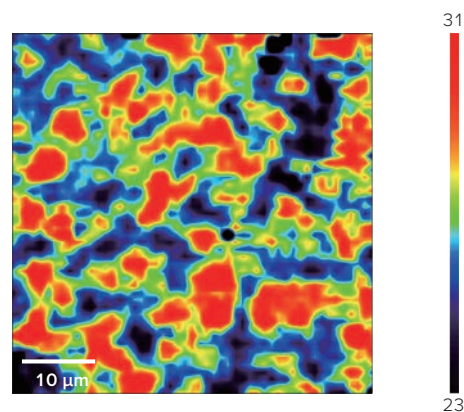
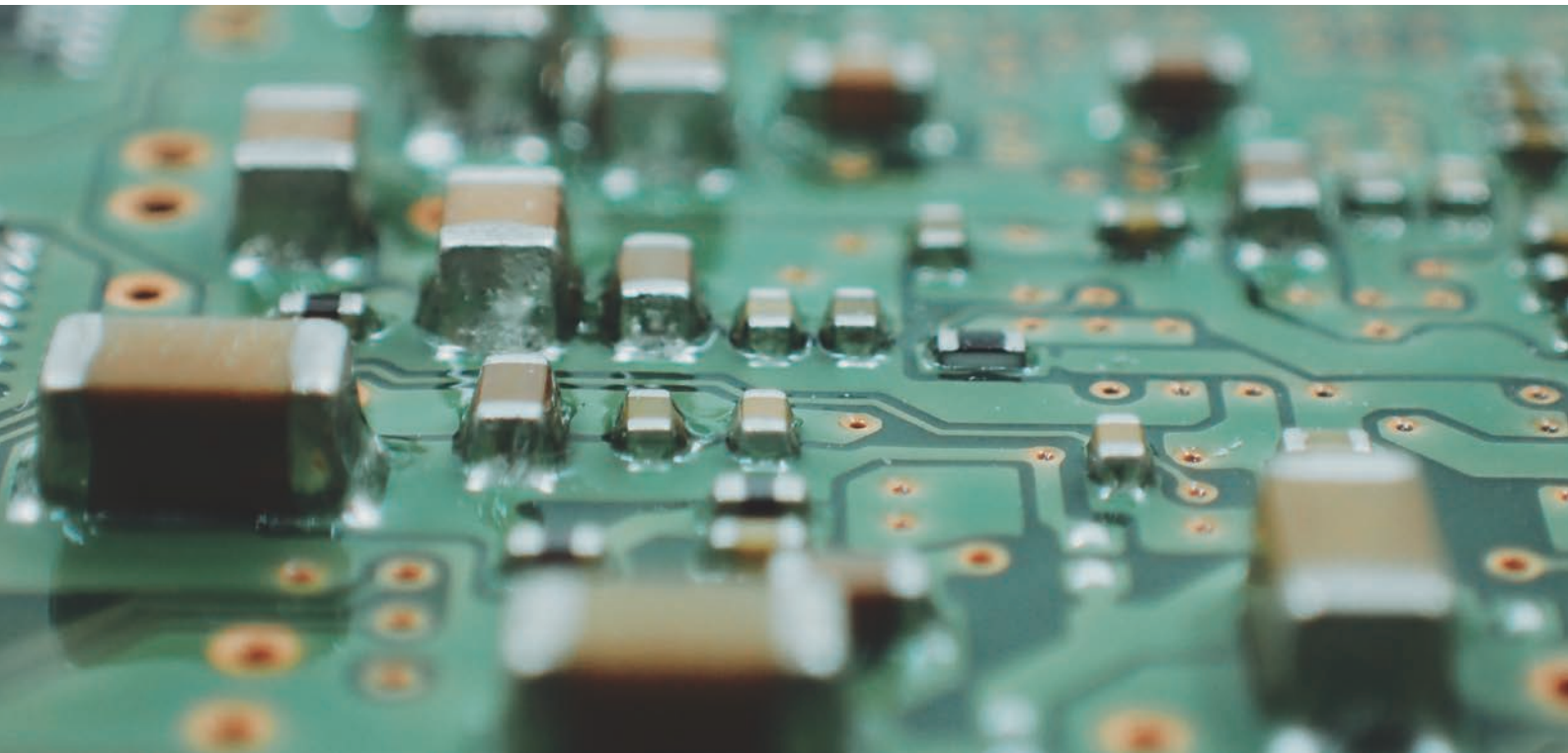


Fig. 7 Raman imaging measurement result. (FWHM of G band)



## Evaluation of Multi-Layer Ceramic Capacitors

Recently, the demands for multi-layer ceramic capacitors (MLCC) have been increasing largely because of the increased use of electronics in automobiles and the implementation of autonomous driving systems as well as the progress of technologies such as 5G, IoT and artificial intelligence (AI).

MLCCs have a structure where the ceramic dielectric and electrodes are stacked alternately, with terminals at the ends, which are used for storing electrical energy (Fig. 1).

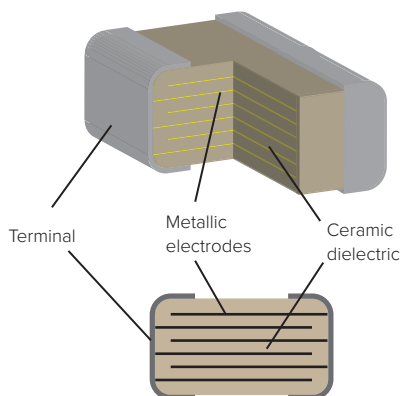


Fig. 1 Multi-layer ceramic capacitor (MLCC) diagram.

Barium titanate ( $\text{BaTiO}_3$ ) is widely used as a ferroelectric material in MLCCs. It is well-known that the phase transition of  $\text{BaTiO}_3$  crystal structure changes with temperature, causing the permittivity to drop dramatically at the Curie temperature. Therefore, it is important to evaluate the quality of  $\text{BaTiO}_3$  to improve its performance and the reliability of MLCCs.

Raman spectroscopy is well suited for the quality evaluation of  $\text{BaTiO}_3$ . It can be used to monitor the changes in crystal structure, since Raman spectra are extremely sensitive to the differences in crystal structure.

This section shows the evaluation of structural change of  $\text{BaTiO}_3$ , and also shows an example of  $\text{BaTiO}_3$  in an MLCC.

### Structural Phase Transition of $\text{BaTiO}_3$ Powder by Heating/Cooling

Temperature-dependent Raman measurements were made of  $\text{BaTiO}_3$  powder (reagent) using a heating/cooling stage (-190 °C to 190 °C) (Fig. 2). The spectral shape changed with temperature, and it was confirmed that the phase transition through 4 different  $\text{BaTiO}_3$  polymorphs occurred. The tetragonal structure which is stable at room temperature (RT) is ferroelectric, and is changed to cubic structure, which is para-electric at temperatures higher than 100 °C. Raman microscopy with a heating/cooling stage can be used to sensitively evaluate the thermal changes in crystal structure.

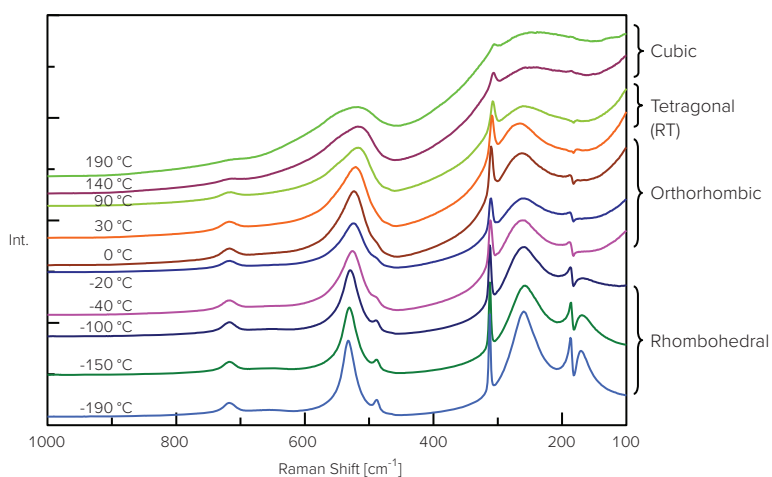


Fig. 2 Raman spectra of heated/cooled  $\text{BaTiO}_3$ .

A heated MLCC cross-section was evaluated using Raman imaging (Figs. 3 and 4). From the results, it is assumed that there were localities of structural change at each point in capacitor.

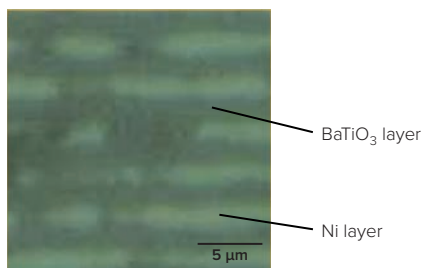


Fig. 3 Observation view.

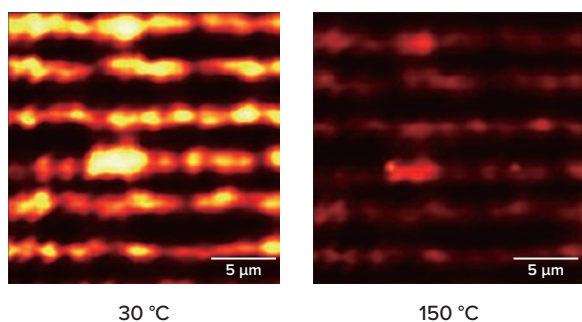


Fig. 4 Raman imaging measurement results at each temperature. (peak area at 520 cm<sup>-1</sup>)

## Evaluating the Deterioration of an MLCC using an Acceleration Test

This section shows the results of deterioration in a MLCC using an acceleration test (Figs. 5 and 6). Raman spectra provide information for evaluating the detailed status (such as crystal structure) of BaTiO<sub>3</sub> layers in MLCC. In addition, Raman imaging provides information about the distribution of deterioration.

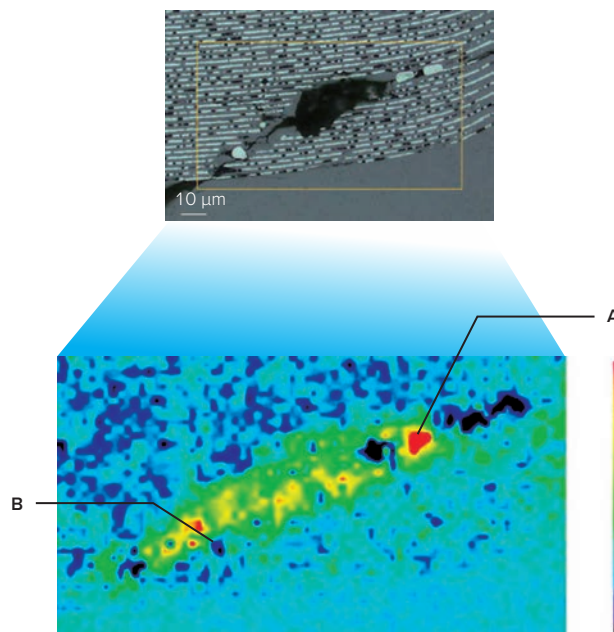


Fig. 5 Observation view and Raman imaging measurement result. (FWHM of 520 cm<sup>-1</sup>)

## Tips

### Heating/Cooling Stage

The optional stage for heating/cooling the sample, depends on the required temperature range. There are several types of stages the user can select. In addition, the dedicated software that controls the temperature provides automated measurement to start from a set temperature, and can also set a heating/cooling ramp and synchronize measurement.



Heating/cooling stage

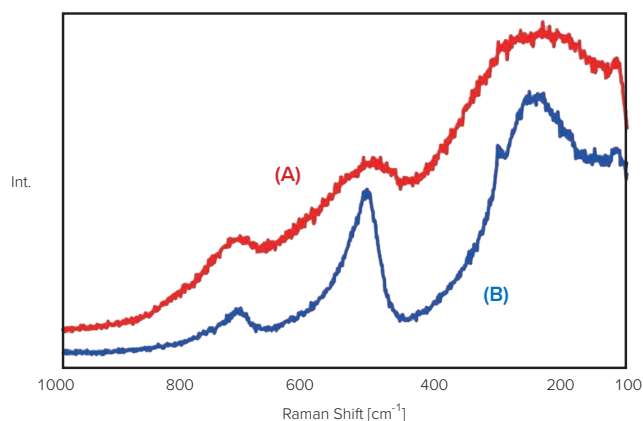
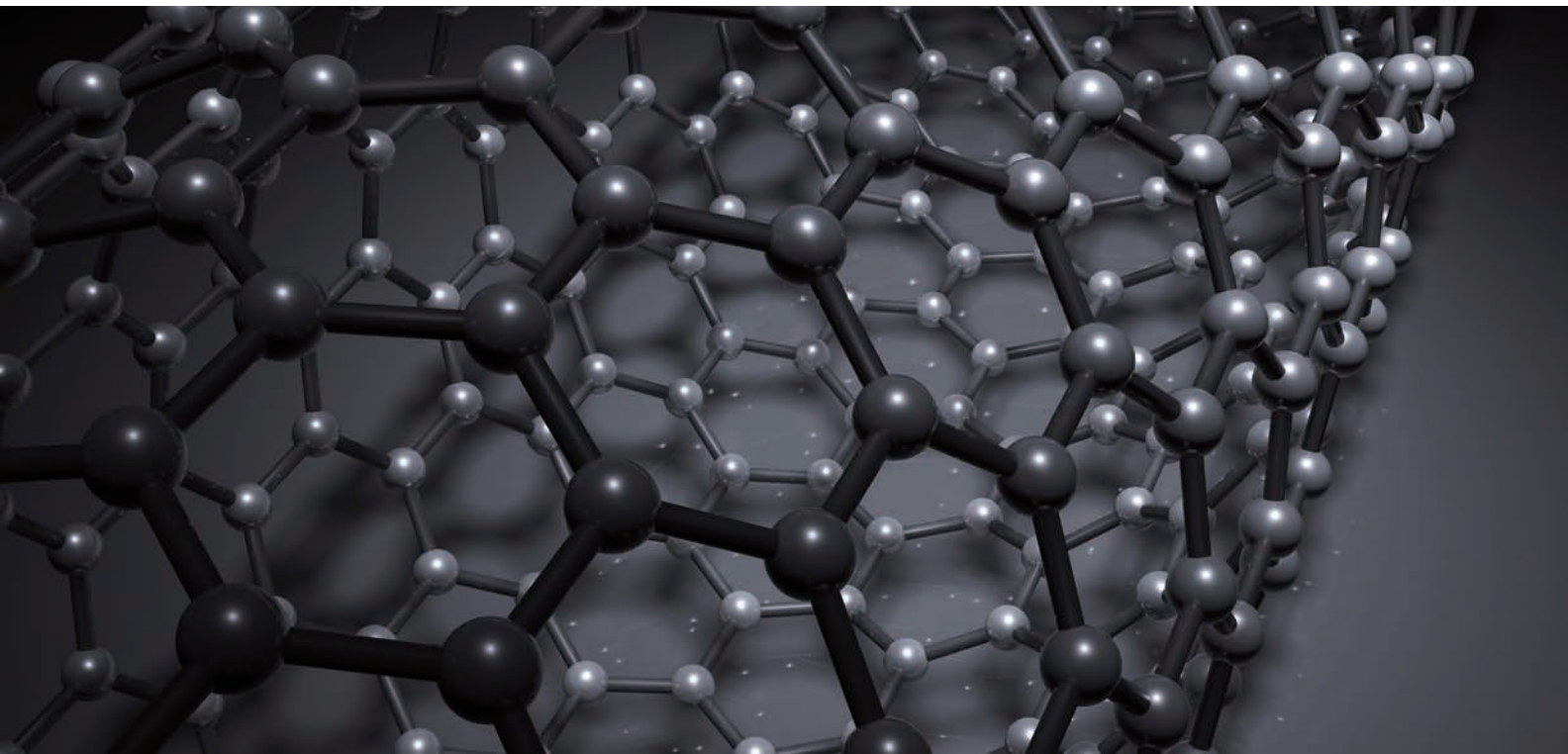


Fig. 6 Raman spectra at each point.



## Evaluation of Carbon Materials

Materials that consist of carbon have various physical properties depending on the bonding between the atoms and their spatial arrangement, which are collectively known as "carbon materials". Utilizing their diverse features, carbon materials are now widely used in different fields. Raman spectroscopy is one of the few methods that can be used to evaluate the physico-chemical properties of carbon materials. Since Raman spectroscopy can measure characteristic spectra of each carbon structure, it can be used to elucidate many of these qualities (Fig. 1).

This section shows examples of carbon materials analyzed using Raman spectroscopy.

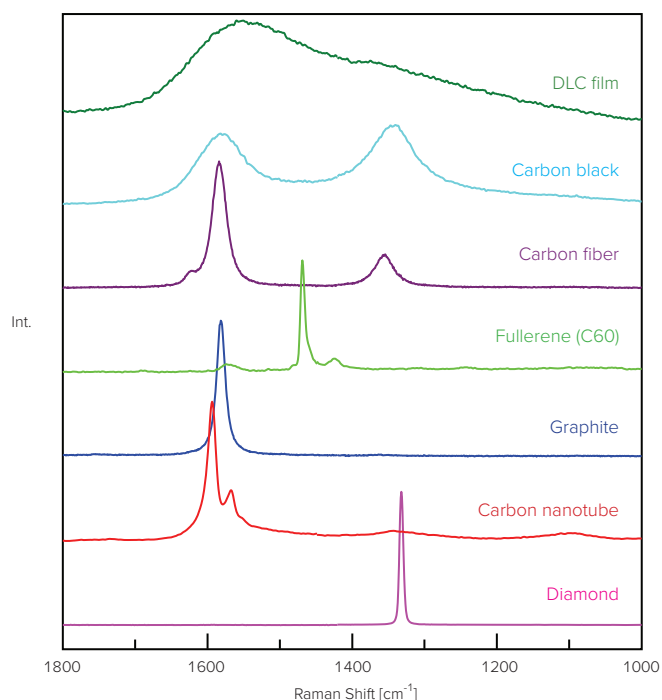


Fig. 1 Raman spectra of each carbon material.

### Raman Imaging of Graphene

Graphene is a single-layer carbon molecule that has a hexagonal honeycomb structure. In comparison with other carbon materials, graphene is a conductor with the following properties: thin, mechanically strong, transparent and flexible. Single-layer graphene, like multi-layer graphene, has a variety of features that have proven to be useful in many applications.

Since the physical (electrical) properties of graphene differ depending on its layer structure, it is important to be able to evaluate this. In addition, during the manufacture of graphene structural defects can occur; a simple and rapid quality control method is required.

Raman spectroscopy can detect the layer structure, defects and edge structure of graphene with great sensitivity. It is well-known that peak shape, width and position of the G' (2D) band (around 2700  $\text{cm}^{-1}$ ) can vary depending on the number of layers, and it can also be applied to the quality evaluation of graphene (Fig. 2). Information about defects and edge structure of graphene can be obtained clearly from the D band (around 1350  $\text{cm}^{-1}$ ) (Fig. 2).

Creating a chemical image of the specified bands provides a visualization of the distribution of the layer structure, defects and edge structure of graphene (Fig. 3).

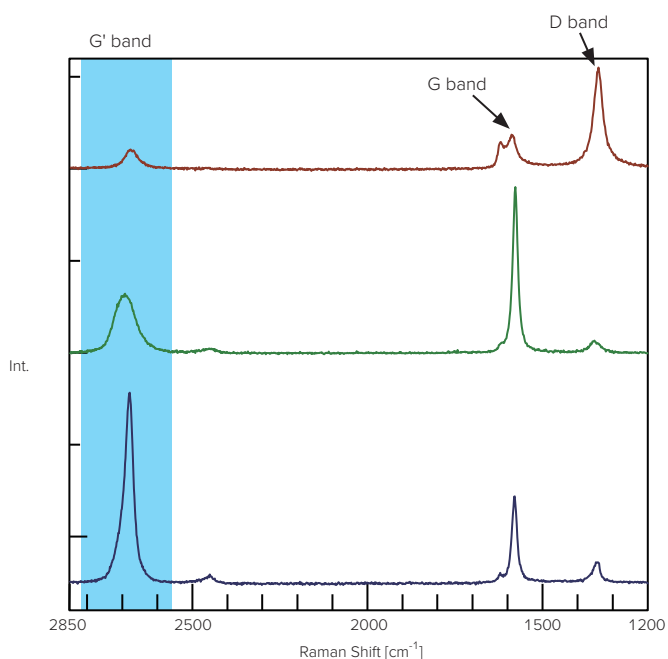


Fig. 2 Raman spectra at each point (graphene).

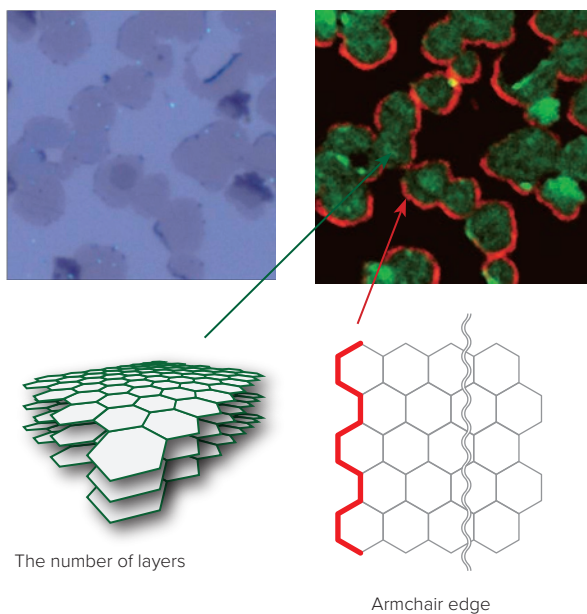


Fig. 3 Observation view (left) and Raman imaging measurement result (right) of graphene. (green: G band, red: D band)

## Evaluation of Carbon Nanotubes in the Low Wave-Number Region

Raman spectroscopy can be applied to the analysis of single-walled carbon nanotubes (SWNTs). SWNTs show characteristics typical to metal and semiconductors due to different electronic structure depending on its chirality and tube radius. Therefore, by exciting the molecules with energy corresponding to the electronic transition (resonance Raman), information about the chirality and tube radius can be obtained.

This section shows the results of Raman measurement of two SWNTs with different methods of synthesis (Samples A and B) (Figs. 4 and 5). In the Raman spectra, three specific bands were observed. The G band (around  $1550\text{ cm}^{-1}$ ) corresponds to the vibrational mode assigned to graphite. In metal SWNTs, a BWF (Breit-WignerFano) type spectrum is observed in the lower wavenumber range of the G band. The D band (around  $1350\text{ cm}^{-1}$ ) is attributed to a defect often used in the evaluation of crystallization. In addition, the band appearing in the low wavenumber region corresponds to the radial breathing mode (RBM), which correlates to the nanotube stretching diametrically, and can be used to estimate the diameter of carbon nanotubes.

(Raman application data: 170-AN-0001)

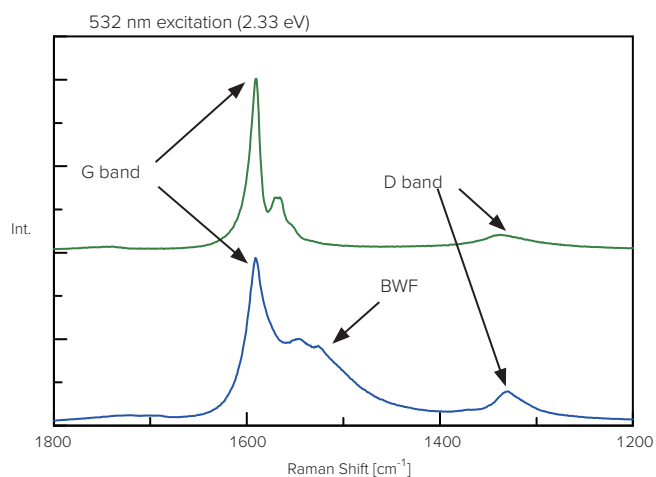


Fig. 4 Resonance Raman spectra of SWNT. (upper: sample A, lower: sample B)

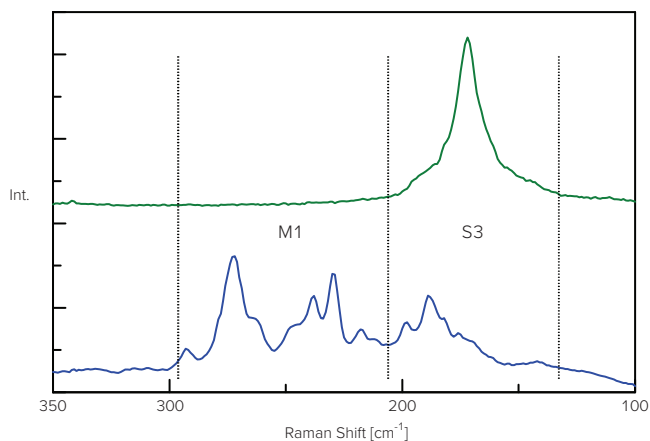


Fig. 5 Resonance Raman spectra of SWNT in the low wavenumber region. (upper: sample A, lower: sample B) (M1: resonance of metallic SWNT, S3: resonance of semiconducting SWNT)

## Excitation Wavelength Dependence of Carbon Nanotubes

In order to verify the dependence on excitation wavelength, Raman measurements of SWNT (Sample B) were performed using several different excitation lasers (Figs. 6 and 7). Using resonance Raman, measurement can be made selectively for specific chirality and tube radius, depending on the excitation wavelength. Therefore, the shape of the Raman spectra changes significantly depending on the selected excitation wavelength. 532 nm excitation is mainly resonant with metallic SWNT, 633 nm with both metallic and semiconducting SWNT, and 785 nm with semiconductor SWNT.

(Raman application data: 170-AN-0001)

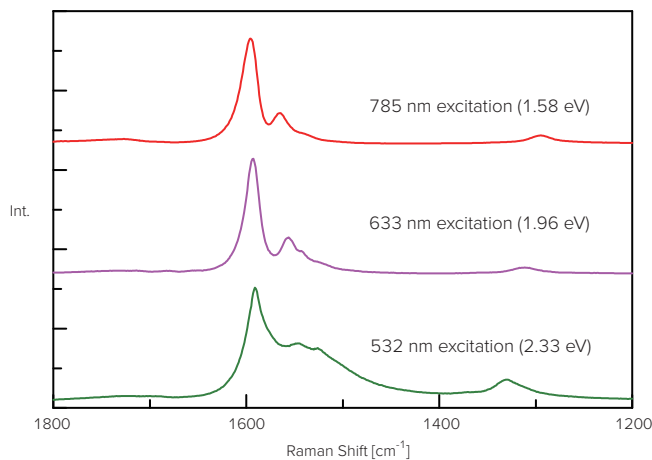


Fig. 6 Raman spectra of SWNT (excitation wavelength dependence).

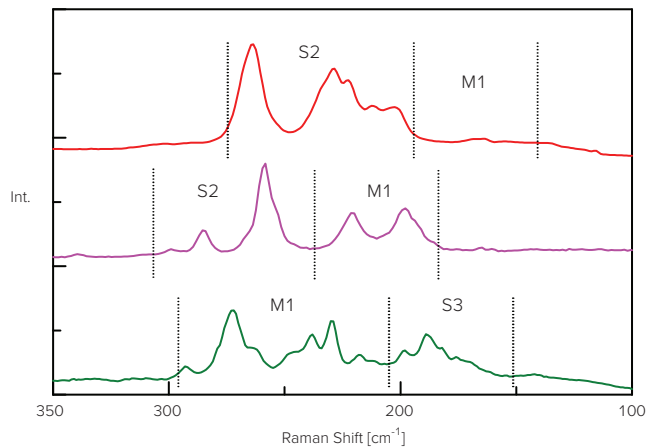


Fig. 7 Raman spectrum of SWNT in low wavenumber region. (excitation wavelength dependence)  
(M1: resonance of metallic SWNT, S2, S3: resonance of semiconducting SWNT)

## Analysis of DLC Coating Distribution of a Blade Edge

Diamond-Like Carbon (DLC) is an amorphous carbon material that has an intermediate molecular structure between diamond and graphite. DLC coatings are used to improve abrasion resistance, chemical resistance etc., and is used as a coating for cutting tools, automotive components, medical equipment, optical components, and many other products.

It is well-known that Raman spectroscopy can acquire structural information about carbon materials (such as DLC, diamond and graphite) with significant sensitivity. The Raman spectrum of DLC consists of a D band (around 1350  $\text{cm}^{-1}$ ) and a G band (around 1550  $\text{cm}^{-1}$ ). Generally, curve fitting to decomposition into G and D bands can be used for evaluating the quality of DLC, such as crystallinity (Fig. 8).

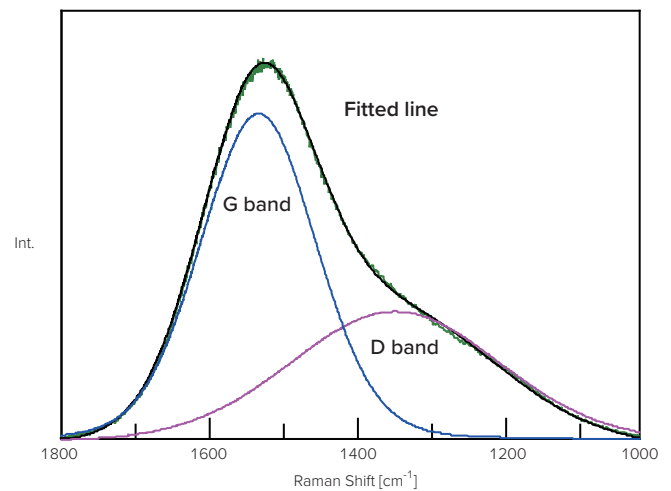


Fig. 8 Decomposition of Raman spectrum (DLC).

As an example, Raman imaging of a DLC-coated blade edge was performed (Fig. 9). Since the sample had a significant slope, measurement was performed using surface scan imaging (SSI), which adjusts automatically to the surface topography (refer to page 23). The results confirmed that there was a DLC coating on the edge of the blade. Creating a chemical image made it possible to visualize the distribution of DLC on the coating.

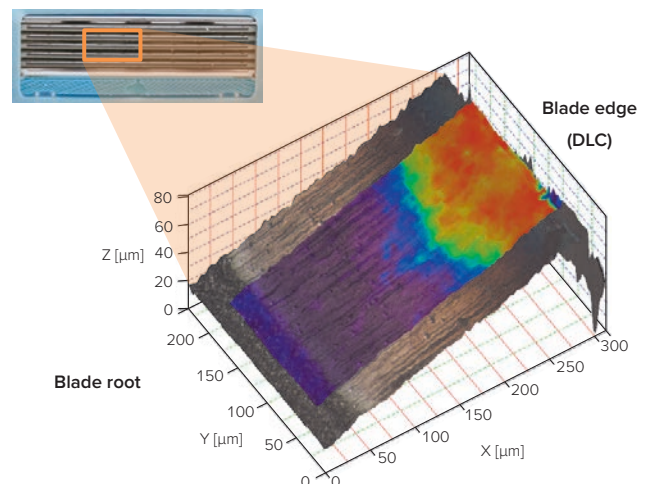


Fig. 9 DLC coating distribution on blade edge.

## Raman Measurement of DLC Coating on Plastic Bottles

### Bottles

DLC coatings have also been used to improve the gas barrier properties of plastic bottles. This section reports the analysis of DLC coated plastic bottles using Raman spectroscopy.

The samples analyzed were two plastic bottles with a visual appearance of slightly different colors (Fig. 10). From this point forward, samples from the slightly colored plastic bottle and from the clear bottle are each referred to as "coated" and "non-coated", respectively.

Measurements were made of both the interior and exterior surfaces of each plastic bottle, and the Raman spectra were compared.



Fig. 10 Measurement sample.

In the case of the non-coated bottle, similar polyethylene terephthalate (PET) spectra were obtained for both interior and exterior surfaces (Fig. 11). For the coated bottle, different spectra were obtained from the interior and exterior measurements (Fig. 12).

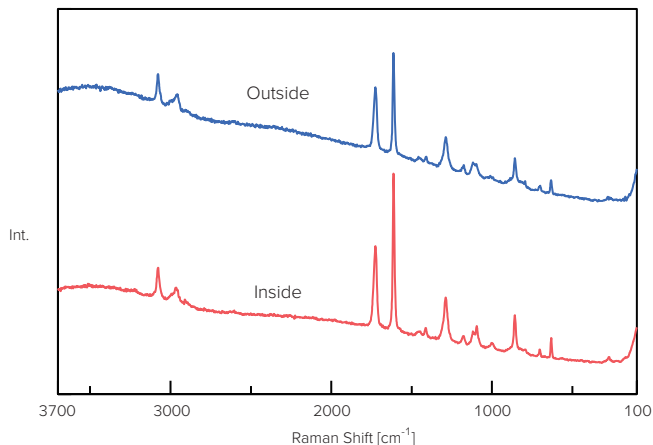


Fig. 11 Measurement of non-coated sample.

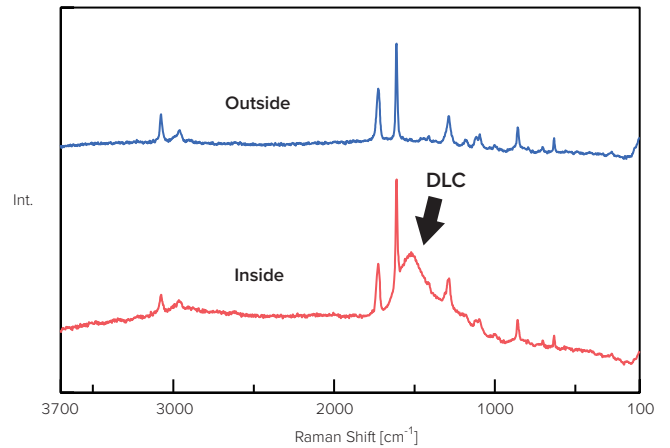


Fig. 12 Measurement of coated sample.

For detailed analysis, a difference spectrum from the coated sample was calculated from both spectra (Fig. 13). A library search identified the difference spectrum as DLC. Only PET was identified on the exterior of the coated sample, but on the interior surface DLC was found in addition to PET, indicating that the inside of the plastic bottle was coated with DLC.

In addition to identification, the quality of the DLC coating can also be evaluated from its spectrum; the D band ( $sp^3$  bonds in the material lattice) and G band ( $sp^2$  bonds in the material lattice) can be deconvolved using curve fitting (Fig. 13). It is possible to evaluate characteristics such as abrasion resistance from the peak positions, half widths, peak ratio etc.

(Raman application data: 020-AN-0023)

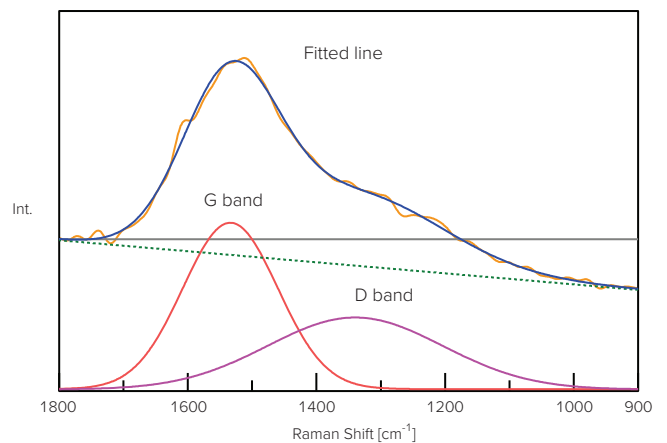


Fig. 13 Difference spectrum of coated sample (Inside – Outside) and D and G bands deconvolution.



## Evaluation of Inorganic Materials

Several inorganic compounds have the characteristic that their physical properties differ depending on crystal structure, and their application in a variety of fields utilizes these characteristics. Therefore, understanding the crystal structures of inorganic materials is important, which can lead to improvements in material quality.

Since Raman spectroscopy excels at measurement in the low wavenumber region, it can be used to observe the specific lattice vibrations that are transmitted through an entire inorganic crystal. This makes Raman spectroscopy a useful tool for evaluating the crystal structure of inorganic materials. In addition, it can also be used to clearly detect the differences in crystal structure, because the lattice vibration varies depending on the arrangement, electric charge, bond length, and bond strength of atoms.

This section shows the evaluation of inorganic materials using Raman spectroscopy.

### Detection of Differences in Crystal Structure in Inorganic Materials

Raman measurements of titania (titanium dioxide,  $\text{TiO}_2$ ) and zirconia (zirconium dioxide,  $\text{ZrO}_2$ ) were performed (Figs. 1 and 2). For both samples, a difference in crystal structure could be discriminated in the low wavenumber region (less than  $800\text{ cm}^{-1}$ ). Since the vibrational frequency of a crystal varies depending on the arrangement of atoms, even if the chemical formula is same, Raman spectroscopy can detect the difference in polymorphs.

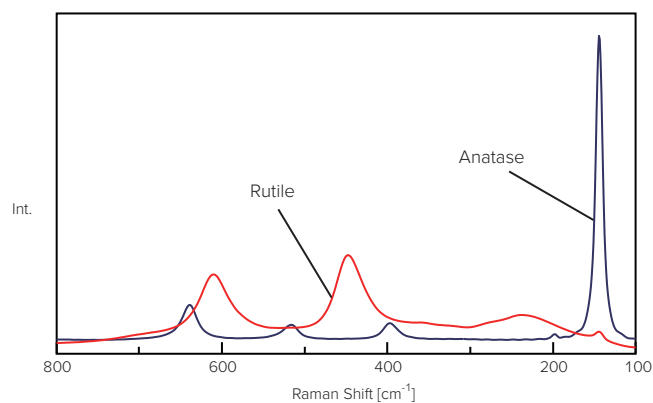


Fig. 1 Raman spectrum of  $\text{TiO}_2$ .

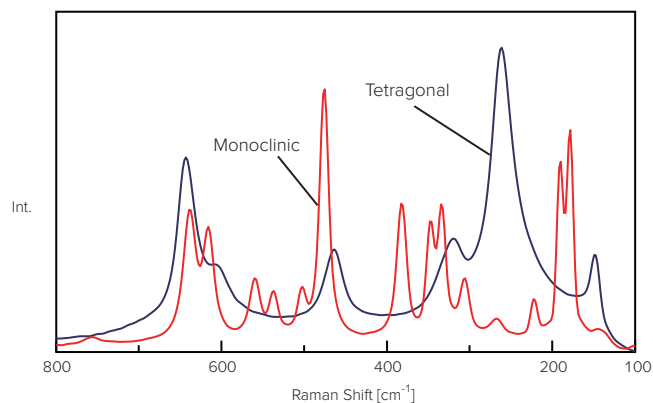


Fig. 2 Raman spectrum of  $\text{ZrO}_2$ .

## Analysis of Surface Iron Oxidation States

Rust that occurs when ferrous materials corrode has various oxidation states and crystal structures, such as  $\text{Fe}_2\text{O}_3$ ,  $\text{Fe}_3\text{O}_4$ , and  $\text{FeOOH}$ , resulting in differences in Raman spectra (Fig. 3). This section shows the analysis of oxidation states on the surfaces of several iron materials using Raman microscopy.

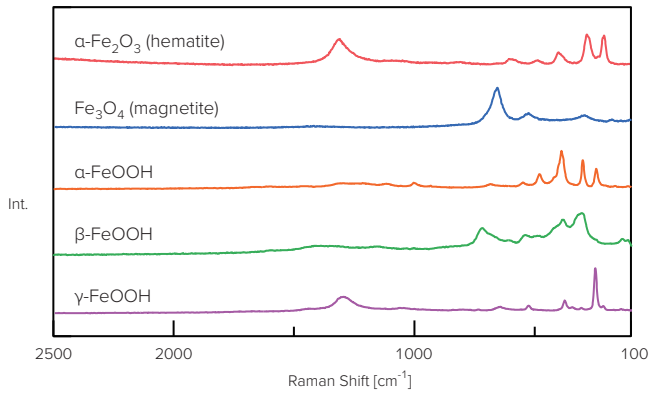


Fig. 3 Raman spectra of iron oxides and hydroxides.

First, Raman measurement was made of a sample collected after environmental exposure (Fig. 4).  $\gamma\text{-FeOOH}$  was mostly detected in this material.

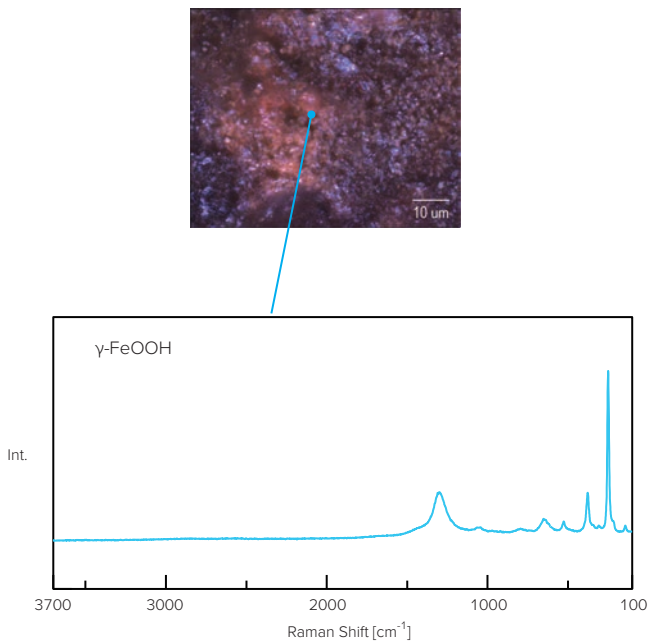
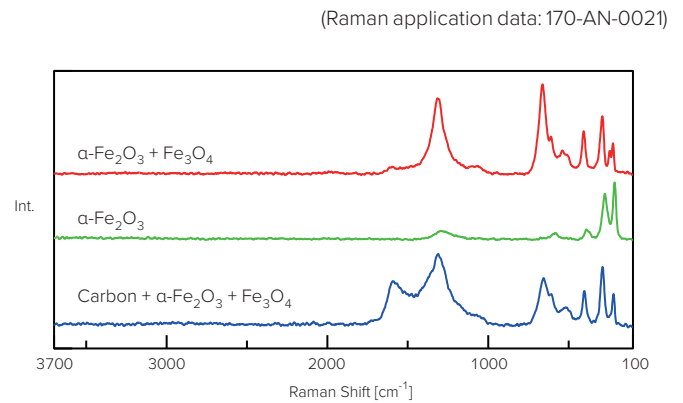


Fig. 4 Measurement result of the sample collected outdoors.

Next, Raman imaging measurement of a sample collected indoors was performed (Fig. 5). Since the surface of the rusted metal had a lot of irregularities, surface scan imaging (SSI) was used for Raman imaging measurement across the irregularities (refer to page 23). In addition, principal component spectra were obtained using multivariate curve resolution (MCR) analysis. Using these as reference spectra, a chemical image of the correlation (similarity) with the reference spectra was created. Three different spectra were obtained, and the component distribution that can be difficult to determine visually was obtained by creating a chemical image.



Principal component spectra and library search results

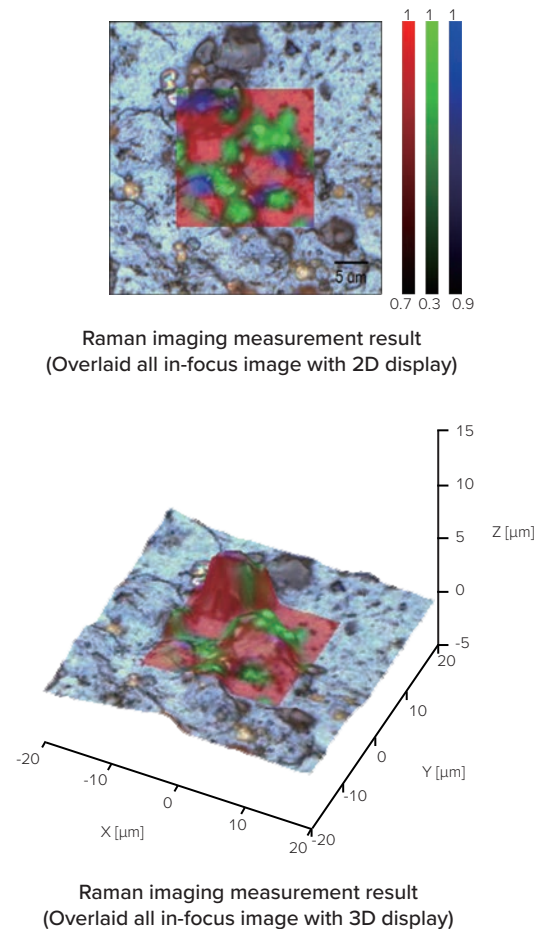


Fig. 5 Measurement result of the sample collected indoors.

# Tips

## SSI (Surface Scan Imaging)

A Raman microscope typically has a confocal optical system, which can obtain Raman spectra with high spatial resolution (sub-micron order). Therefore, it can be applied to the characterization of minute foreign material (down to 1  $\mu\text{m}$ ) and extremely thin layers. However, due to the high spatial resolution of the Raman microscope, slight focus deviation on the measurement surface greatly affects the intensity of the spectrum. As a result, Raman imaging of a sample with an uneven or sloping surface may not provide results.

In order to solve this problem, JASCO developed surface scan imaging (SSI). SSI acquires the surface shape information of the sample as a data matrix of the corresponding height of the stage prior to measurement (Fig. 6). Measurement is made while the focal point is controlled by the stage height following the surface shape, not by auto-focus. By using SSI, samples with uneven surfaces, which have previously been difficult to measure, can now be imaged using Raman microscopy with high S/N.

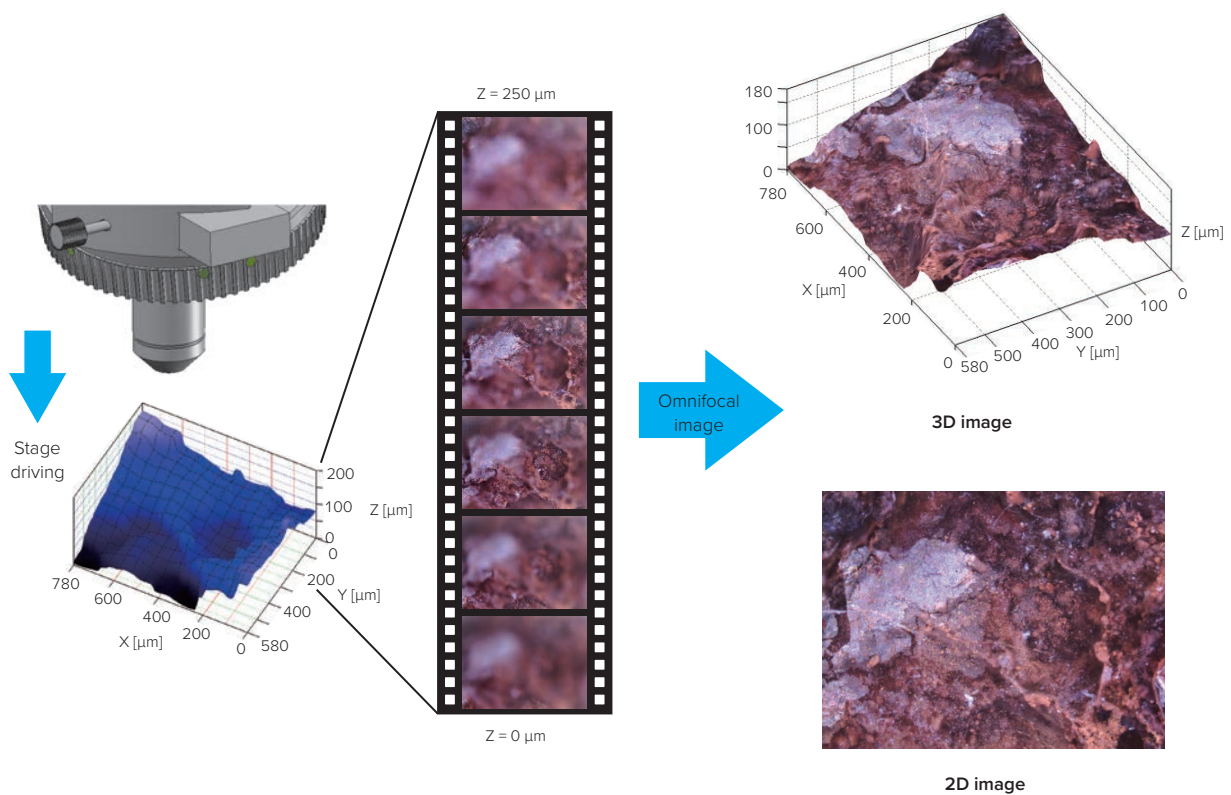


Fig. 6 Imaging of an uneven surface using omnifocus (SSI).



## Evaluation of the Physical Properties of Polymers

Products manufactured from polymers rarely consist of a single component; combining different polymers can produce materials with superior properties. Therefore, to understand the qualities of polymer materials, it is important to obtain information that simple visual observation cannot provide.

Raman spectroscopy is used to identify the components in a material without destroying the sample and can also determine information about crystallinity. In addition, the physical properties of blended polymers depend on the mixture of ingredients. Raman imaging provides information about component distribution, which cannot be obtained by visual observation. Raman spectroscopy can also be used to analyze the layers in polymer laminates.

This section shows the evaluation of polymer materials using Raman spectroscopy.

### Visualization of Sea-Island Structure of a Polymer Blend

Blending several polymers can create functional resin materials with superior physical properties. It is known that the sea-island structure is formed depending on the affinity between the polymers, and its distribution depends on their mechanical properties.

Raman imaging measurement of the surface of a commercially available Acrylonitrile Butadiene Styrene (ABS) resin (20  $\mu\text{m}$   $\times$  20  $\mu\text{m}$  region) was performed, and the distribution of two principal components (butadiene and acrylonitrile styrene) was visualized using multivariate curve resolution (MCR) analysis (Fig. 1). Raman imaging measurement can visualize the composition distribution, which cannot be seen in the observation view.

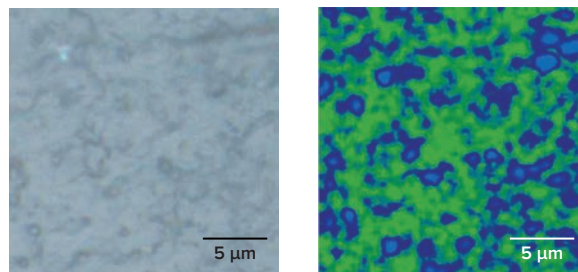


Fig. 1 Observation view (left) and Raman imaging measurement result (right). (blue: butadiene, green: acrylonitrile styrene)

### Evaluation of Crystallization in a Micro Area on a Plastic Bottle

The Raman spectrum of polyethylene terephthalate (PET) (Fig. 2) measured with a full width at half maximum (FWHM) of the carbonyl group ( $1730\text{ cm}^{-1}$ ) correlates well with the crystallization density<sup>9)</sup>. This section shows the evaluation of the distribution of crystallization in a cross-section of a plastic (PET) bottle.

Two samples of a bottle were made, then a cross-section of each was prepared using a slicer (location A and B) (Fig. 3), an HW-1 variable angle slicer (JASCO Engineering Co., Ltd.) was used to make good cross-section samples.

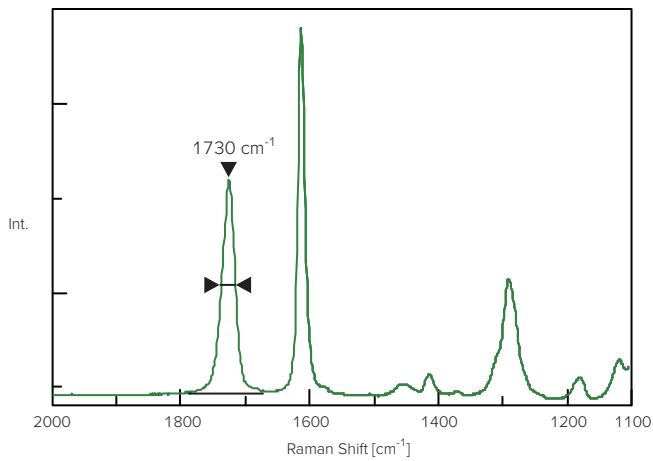


Fig. 2 Raman spectrum of PET.

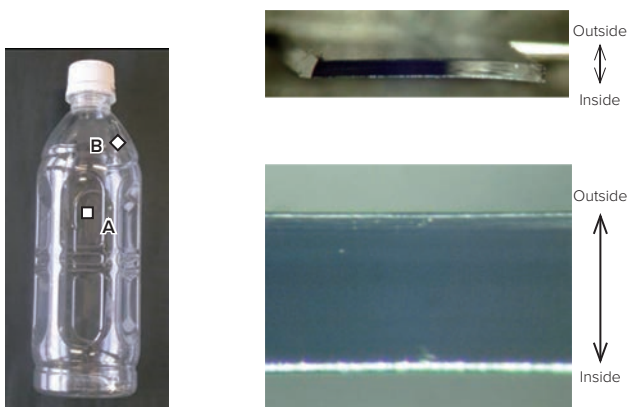


Fig. 3 Sampling part and its cross-section.

## Non-Destructive Depth Profile Measurement and MCR Analysis of Polymer Laminate

Stacking several polymers with different properties can produce a polymer laminate with valuable functionality such as heat resistance, heat sealability, high rigidity, flexibility, cold resistance and easy-peeling. Since the component distribution in each layer affects the overall functionality of polymer laminates, it is important to confirm that the material can be manufactured to the intended design.

Raman spectroscopy can perform non-destructive depth profile measurement without having to make a cross-section of the sample. In addition, utilizing multivariate curve resolution (MCR) analysis, the components in each layer can be easily identified, and their distribution can then be visualized.

In order to verify the structure, non-destructive depth profile measurement of a polymer laminate was performed (Figs. 5 and 6). Different layers were clearly identified because of the improved spatial resolution offered by JASCO's unique confocal optical system - Dual Spatial Filtration (DSF) (refer to page 7). MCR analysis confirmed that each observed layer agreed very well with the actual product design.

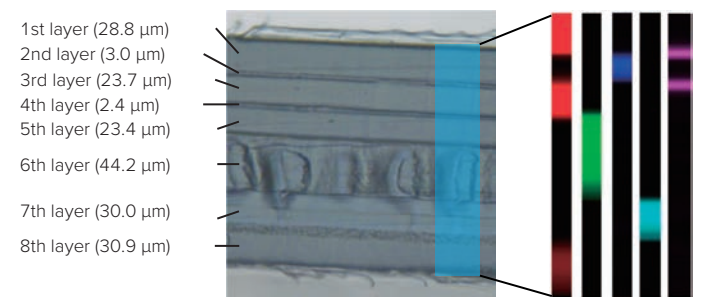


Fig. 5 Sample overview (cross-section, left) and component distribution (right). (red: polypropylene, green: polyethylene, blue: cellulose, aqua: polyamide, purple: polyurethane)

Multi-point measurement was carried out at 50 μm steps through the sample section, and the FWHM of the carbonyl group was calculated at each depth (Fig. 4). The FWHM and crystallization show a negative correlation: as the amount of crystallization increases the FWHM becomes narrower. It was confirmed that both crystallization distributions differ from each other.

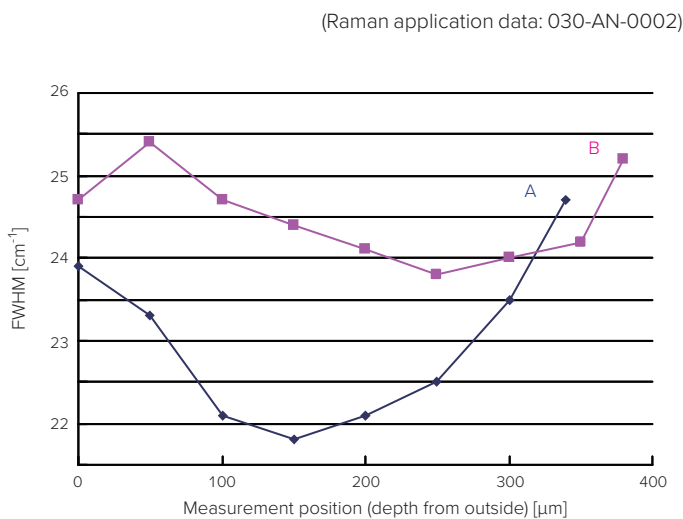


Fig. 4 FWHM calculation results in 1730 cm<sup>-1</sup>.

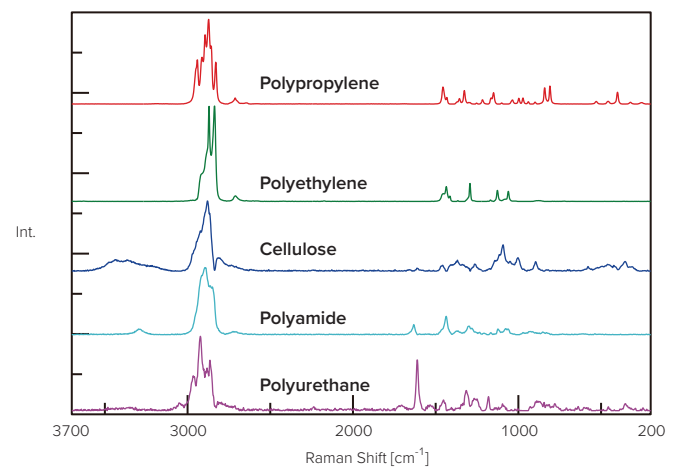


Fig. 6 Five principal component spectra and library search results. (obtained by MCR analysis)

1) Ian R. Lewis, Howell G. M. Edwards, *Handbook of Raman Spectroscopy* (Marcel Dekker, INC., 2001).

## Evaluation of the Orientation of Polyethylene by Raman Spectroscopy

Plastic string has the property of easily tearing in its cross section, but with strength in the longitudinal direction. This is because stretching the fibers orients the molecular chains, resulting in increased physical strength in that direction. This section reports the orientation analysis of a polyethylene string using polarization measurement with a Raman microscope and IQ Frame (refer to page 29).

A polyethylene string was fixed to a metal plate and set in the IQ Frame. For polarization measurement, the analyzer (polarizer) was placed so that the sample was parallel to the polarization of the incident light (laser), and Raman scatter polarized parallel to the incident light was detected. The sample was rotated in 10° steps using the scale on the IQ Frame, and Raman spectra were acquired at each of the 36 points (total 360°) using the rotational alignment function of the IQ Frame. It was confirmed from the observed image that the same point could be measured at each angle (Fig. 7).

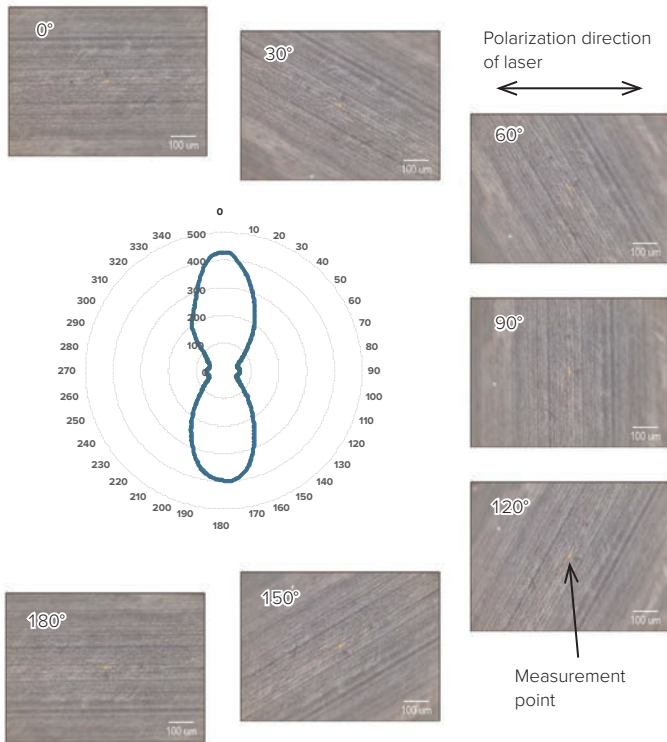


Fig. 7 Peak intensities plot and observation view.

As a result of obtaining Raman spectra by rotating the polyethylene string through 360°, changes were observed in the C-C skeletal vibration (Fig. 8). The C-C skeletal vibration is closely related to the degree of orientation. By plotting the peak intensities at each angle, it was confirmed that a figure-8 shaped intensity distribution with maxima at 0° and 180° were observed (Fig. 7). Therefore, it is suggested that this polyethylene string sample was strongly stretched uniaxially in the laser polarization direction (horizontal direction on the page) at 0° and 180°.

(Raman application data: 030-AN-0024)

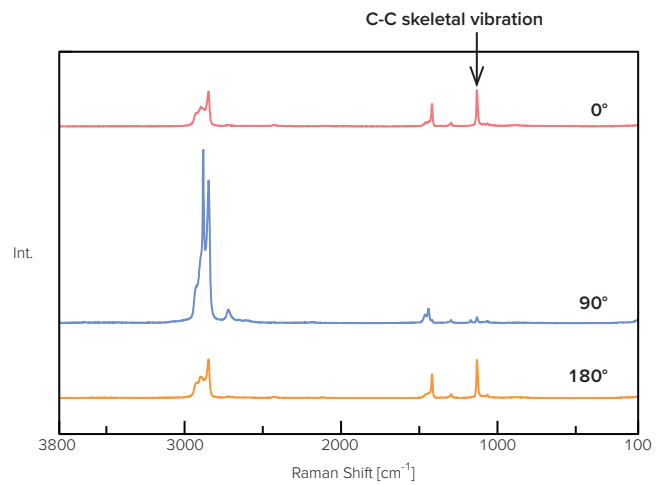
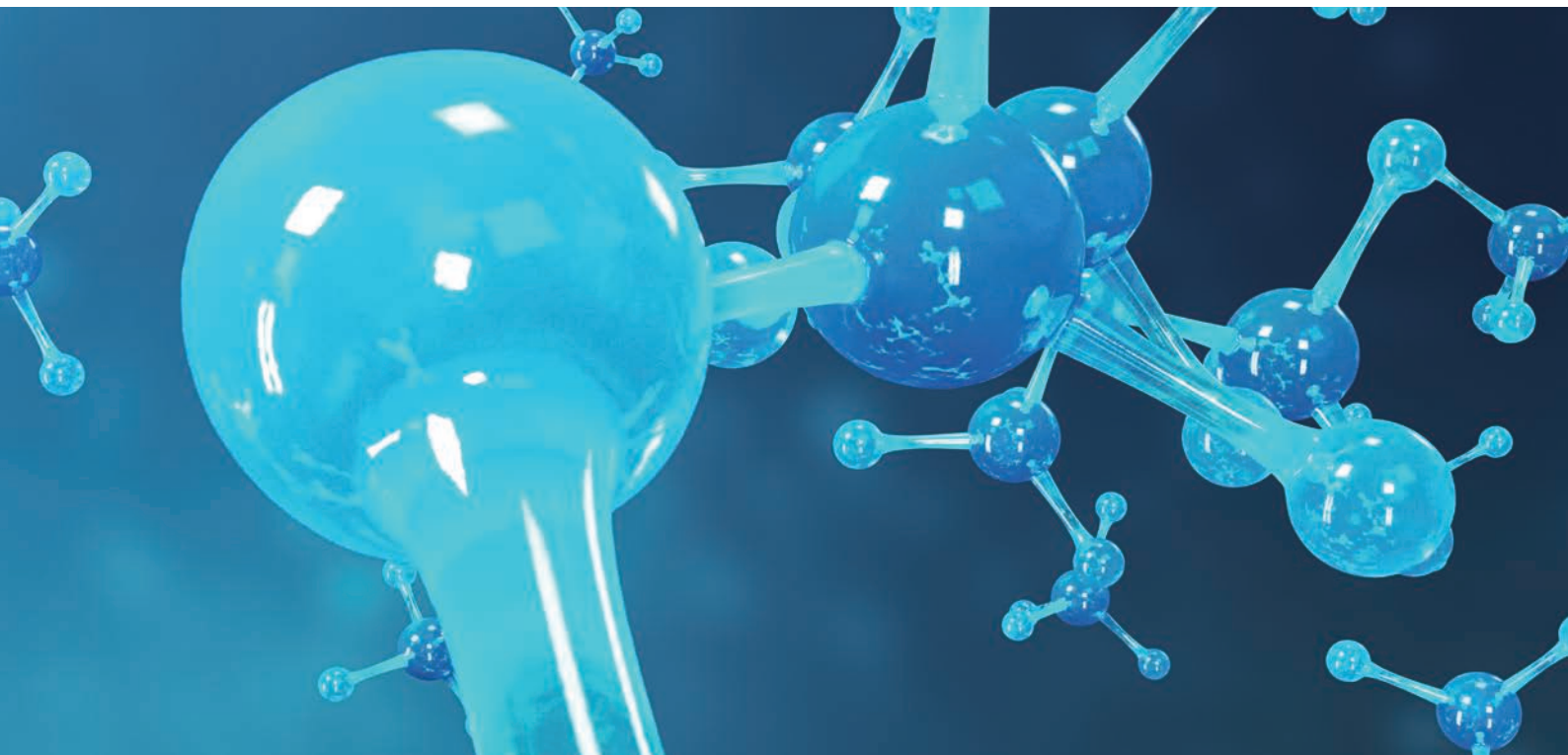


Fig. 8 Raman spectra at 0°, 90° and 180°.



## Analysis of the Orientation and Secondary Structure of Spider Silk

Spider silk is a remarkable protein material with a tensile strength greater than that of steel, while at the same time being more ductile than nylon. Spider silk is attracting attention as a source of next generation materials. It exhibits partial crystalline properties where the protein molecules are oriented parallel to the fiber axis during self-assembly. The aggregation of certain amino acid residues in the silk dictates the elasticity and strength of the material; as a result there are various types of spider silk. A typical orb web is composed of three fibers each with different physical properties - dragline, radial line and spiral line (Fig. 1). This section reports the structural analysis of spider silk proteins by polarization measurement with a Raman microscope.

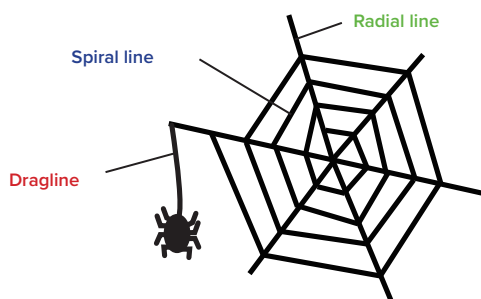


Fig. 1 Example of spider silks.

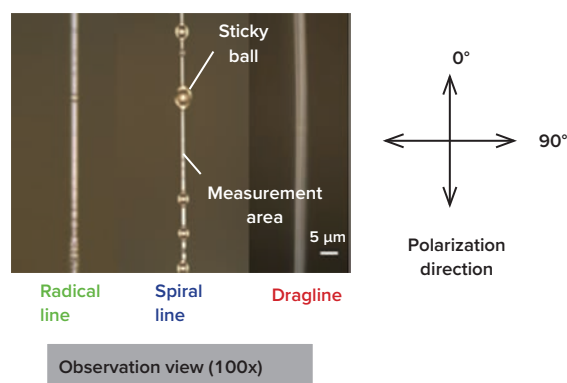


Fig. 2 Definition of polarization direction.

First, polarization measurements using a Raman microscope were performed (Fig. 3). These show the differences in protein orientation, secondary structure, and amino acid composition. The amide I and amide III bands are characteristic of protein peptide bonds, which vibrate in the direction perpendicular and parallel to the molecular axis, respectively, so that their peak intensity ratios reflect the magnitude of protein orientation. In addition, it is well known that the peak positions of amide I and amide III shift due to differences in the secondary structure of proteins<sup>1</sup>.

Raman measurements were performed for each of the three types of spider silks (dragline, radial line, and spiral line) with diameters of several  $\mu\text{m}$ , which were sourced from the oriental golden orb web spider, *Nephila clavata*. Measurements were performed by rotating the spider silk to align the polarization direction of the laser light with the axis parallel to, and orthogonal to the fiber axis (Fig. 2).

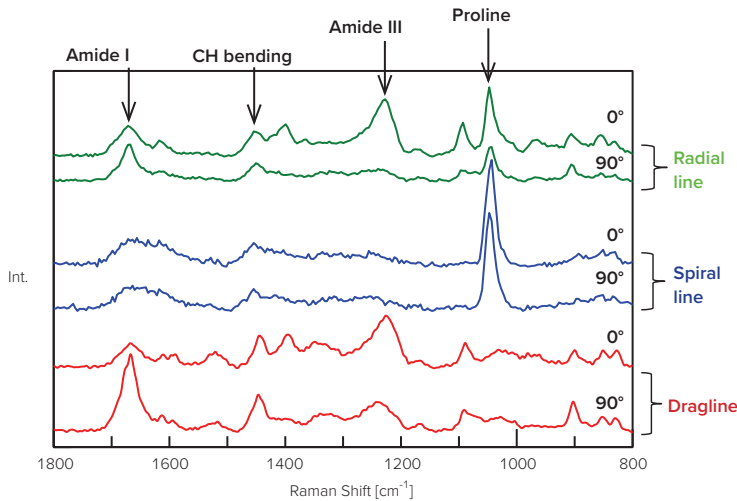


Fig. 3 Polarization measurements of each spider silk.

Analysis of the peak intensity ratio and peak position of amide I and amide III show that the dragline and radial line proteins are largely oriented in the fiber axis direction and contain a large crystalline component with  $\beta$  sheet structure. This is thought to be related to the tensile strength of the spider silk in the direction of the fiber axis.

The spiral line (for catching prey) has low orientation and contains many  $\alpha$  helices and random coil structures. This is thought to be related to the ductile and elastic properties of the spiral line fiber (Fig. 4). In addition, the spectrum of the spiral line fiber suggests that its surface includes proline-rich 'sticky-ball' components.

(Raman application data: 210-AN-0019)

This application is the result of a joint research project with Prof. N. Katayama at the Graduate School of Natural Sciences, Nagoya City University.

1) Carey, P. R., *Biochemical Applications of Raman and Resonance Raman Spectroscopies*, (Academic Press, New York, 1982).

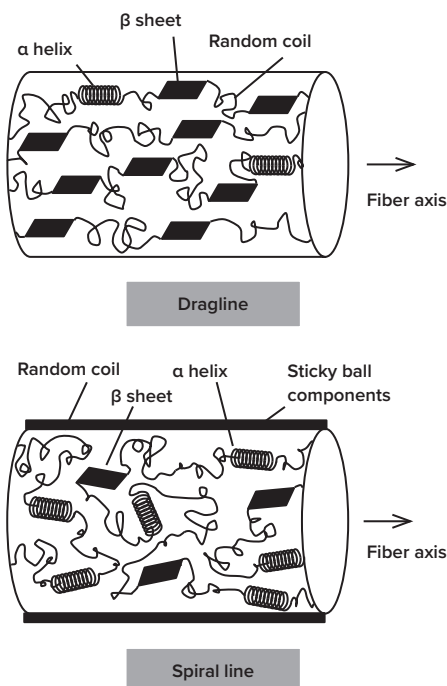


Fig. 4 Image of dragline and spiral line silk fibers.

# Tips

## Polarization Measurement using IQ Frame

The functions and properties of polymer materials such as films and chemical fibers are closely related to the molecular orientation. Non-contact, non-destructive evaluation of the orientation of polymers can be made to micron resolution using polarization measurement with a Raman microscope.

When performing the polarization measurement by rotating the sample, it is not easy to move the sample to exactly the same measurement position after rotating it under the Raman microscope (Fig. 5).

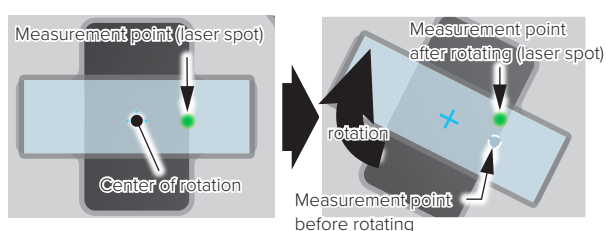


Fig. 5 Conventional polarization measurement.

In order to satisfy the above needs, JASCO has developed a unique solution - IQ Frame, which includes the image matching technology (Fig. 6). IQ Frame uses image matching to perform the measurement at exactly the same position even after rotating the sample (Fig. 7). IQ Frame makes it possible to perform polarization measurement without changing the polarization plane of laser. Since the plane of polarization plane of the laser beam is not changed, a spectrum can be acquired without the polarization influences of optical elements in the spectrometer. By continuously rotating the sample, it is possible to draw a profile of peak intensity.

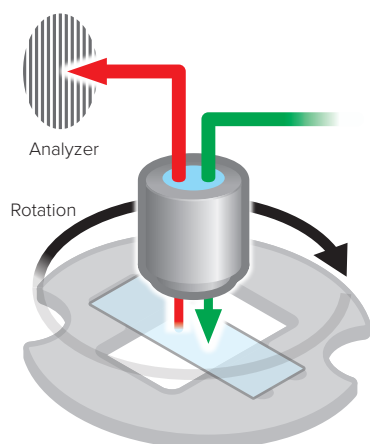


Fig. 6 Polarization measurement using IQ Frame.

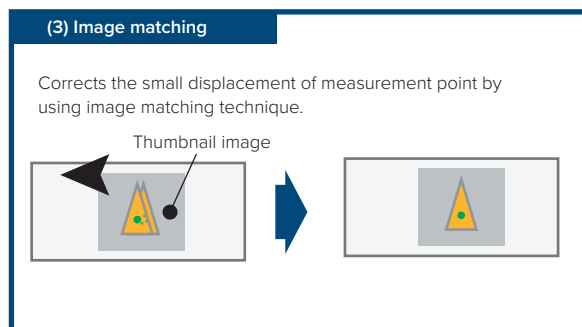
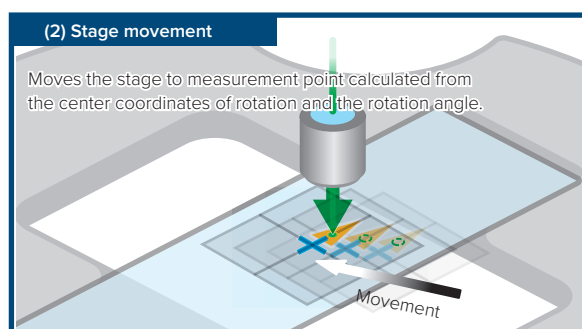
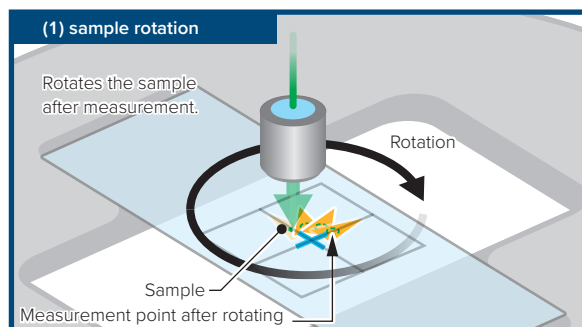
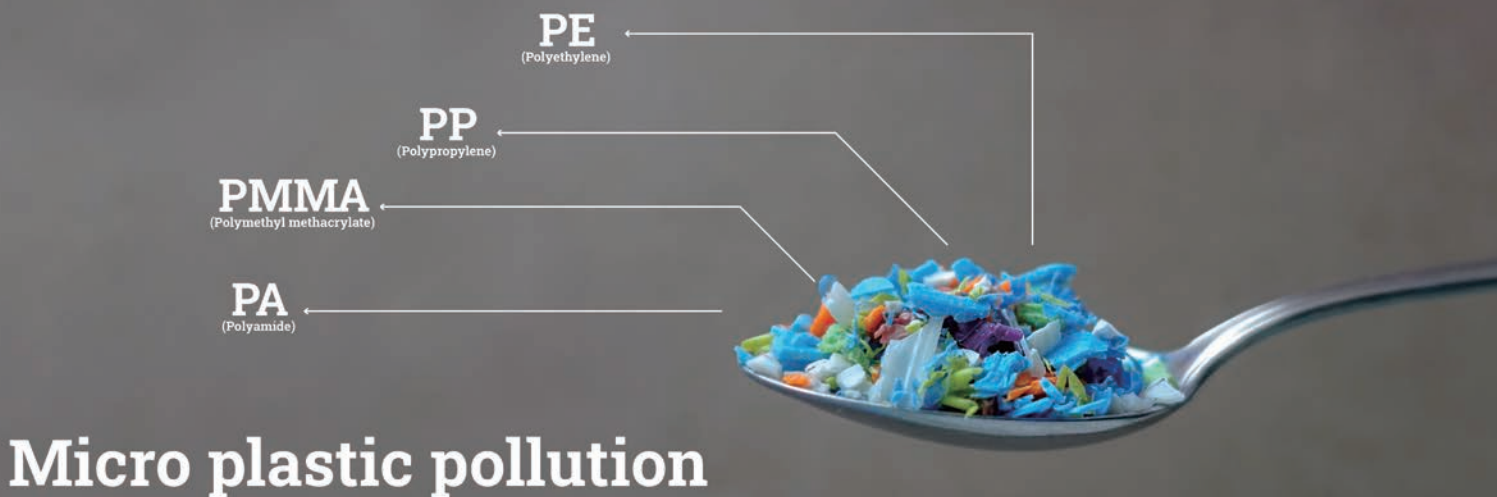


Fig. 7 Measurement overview (after rotating).



## Analysis of Microplastics

Microplastics are a major global problem; this form of environmental pollution is not only found in just about every type of water source on the planet, it can also be found throughout the food chain with potential for damage to life on Earth. Recently, the investigation into microplastics has exploded with scientists around the world assessing the distribution and effects of these materials with a view to reduce the environmental impact and understand the widespread implications.

This section shows examples of the evaluation of microplastics using Raman spectroscopy.

### Analysis of AMPs

Airborne microplastics (AMPs, PM<sub>2.5</sub>) were collected on an aluminum oxide membrane filter at the top of Mt. Fuji (in the free troposphere) at night. These were analyzed using Raman microscopy (Figs. 1 and 2). Polyethylene terephthalate (PET) and Polyhydroxybutyrate (PHB), a biodegradable plastic, was found as particulates, with sizes around 5 μm or less. The results demonstrate that Raman microscopy is well suited for microplastics analysis.

(Raman application data: 100-AN-0031)

We would like to express our sincere gratitude to Professor Hiroshi Okochi, School of Creative Science and Engineering, Waseda University, Japan, for providing the AMPs samples and for his guidance.

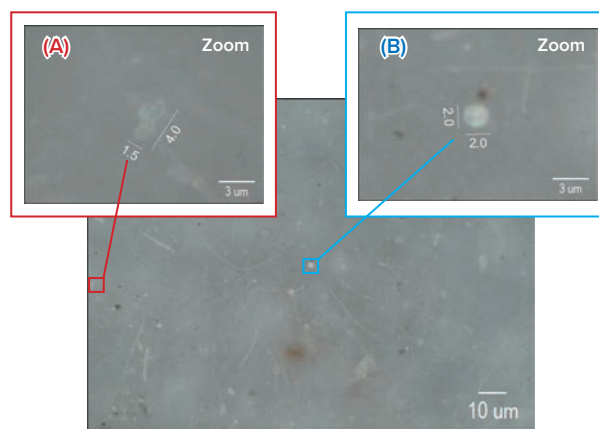


Fig. 1 Observation view.

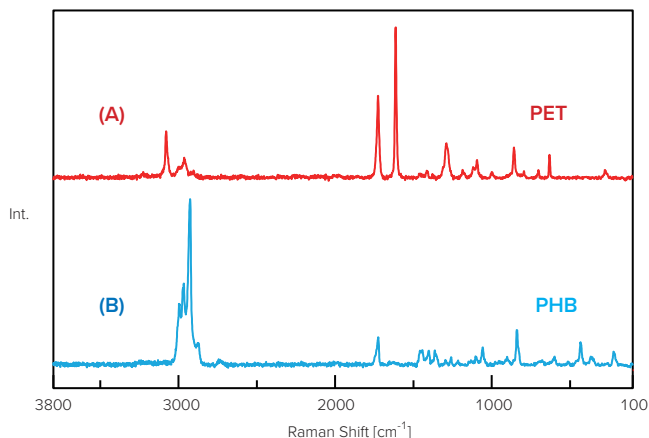


Fig. 2 Measurement results.

## Combined IR/Raman Analysis of Plastic Particles

Measuring a sample using two complementary analytical methods (such as Raman spectroscopy and IR spectroscopy) can provide more information than one single method, and it can also increase confidence in the results. When performing combined analysis, IQ Frame makes sample measurement using different spectroscopic techniques much more user-friendly (refer to page 33) (Fig. 3). This section shows a sample evaluation using IQ Frame with IR and Raman microscopes.

### Raman Microscope



### IR Microscope



Fig. 3 IQ Frame overview.  
(between Raman microscope and IR microscope)

A sample sprayed with plastic particles were measured using Raman and IR microscopy (Fig. 4).

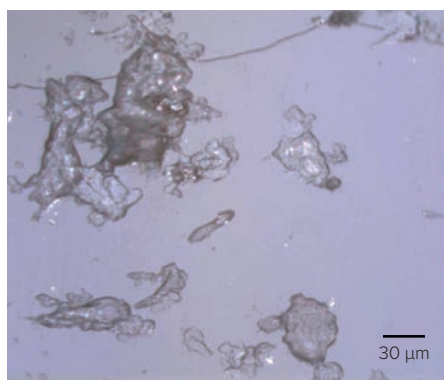
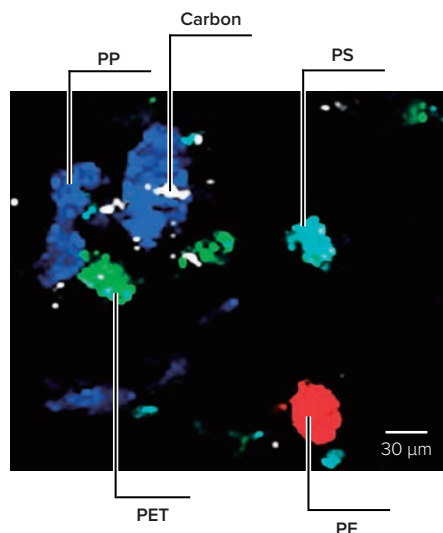
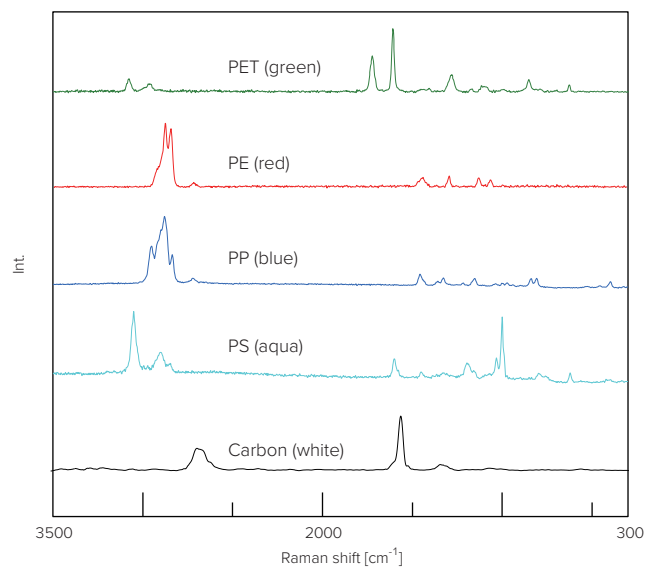


Fig. 4 Observation view.

First, Raman imaging measurement was performed (Fig. 5). Principal component spectra were obtained using multivariate curve resolution (MCR) analysis, and a chemical image was created using the specified bands in the principal component spectra. As a result, carbon was found in addition to four plastics identified by Raman spectroscopy: polyethylene terephthalate (PET), polyethylene (PE), polypropylene (PP) and polystyrene (PS).



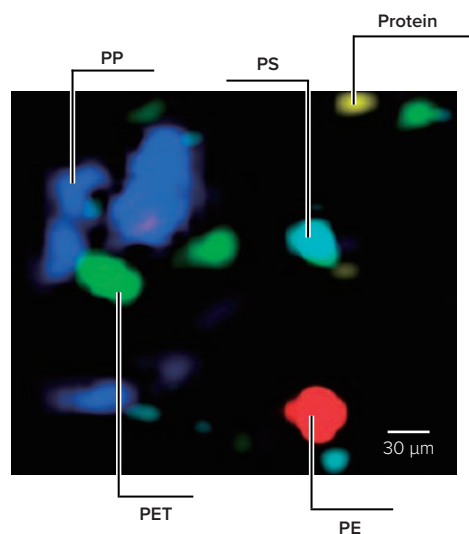
Raman imaging measurement result  
(peak heights of the specified bands)



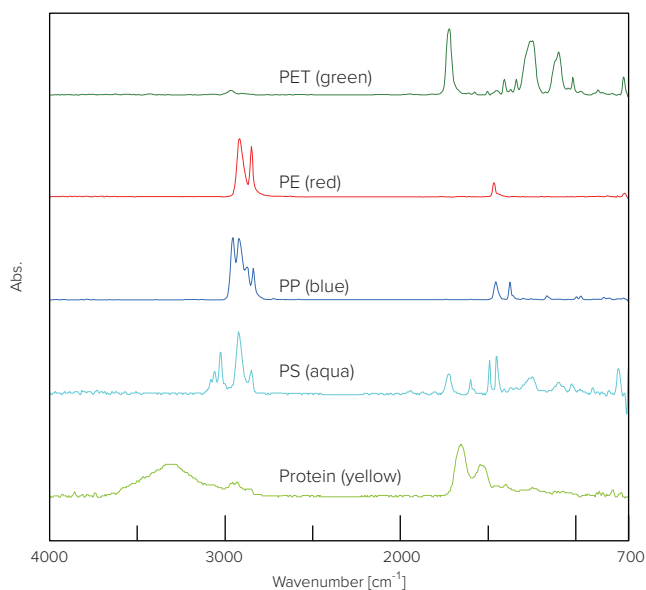
Principal component spectra

Fig. 5 Measurement result (Raman microscope).

Next, utilizing IQ Frame, IR imaging measurement was performed at exactly the same position measured using the Raman microscope (Fig. 6). The principal component spectra were obtained by MCR analysis, and a chemical image was created using the principal component spectra. As a result, protein was found in addition to four plastics: PET, PE, PP and PS.



IR imaging measurement result  
(score of the principal component spectra)



Principal component spectra

Fig. 6 Measurement result (IR microscope).

Only five components could be detected using either IR or Raman spectroscopy alone. However, combining analysis from both techniques resulted in six different components being detected.

In order to visualize the complete information, both chemical images were overlaid (Fig. 7). This showed the protein detected by IR spectroscopy together with the other five components, PET, PE, PP, PS and carbon detected by Raman spectroscopy.

These results indicate that using the strong points of both IR/Raman spectroscopy can be combined to be more useful than a single analytical technique alone.

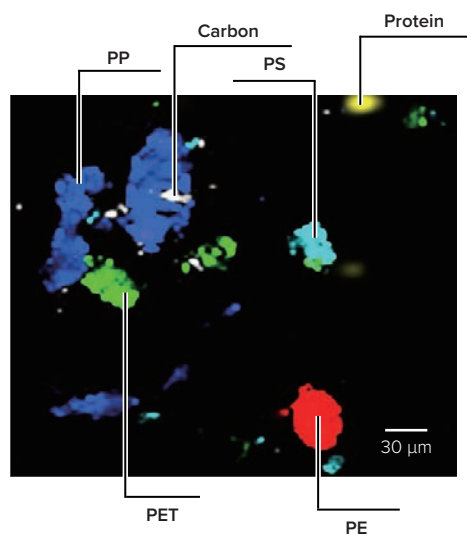


Fig. 7 Overlaid chemical image of Raman and IR.

In the analysis by Raman microscopy, carbon was detected in addition to the four plastics, whereas in the analysis by IR microscopy, protein was detected (carbon could not be detected). These results were obtained because Raman spectroscopy has low detection sensitivity for protein, but it is also good for carbon analysis.

# Tips

## Combined Analysis by IQ Frame

JASCO offers micro-spectroscopy systems for acquiring information at a coordinated location (including Raman, IR and UV/Vis micro-spectrophotometers). Each technique by itself yields useful information, but in order to obtain additional information about materials, demands for combined evaluation using spectroscopic techniques are increasing.

However, it is not easy to measure samples at the same position between different microscopes.

In order to satisfy the above needs, JASCO has developed a unique solution IQ Frame including image matching technology (Fig. 8).



Fig. 8 IQ Frame.

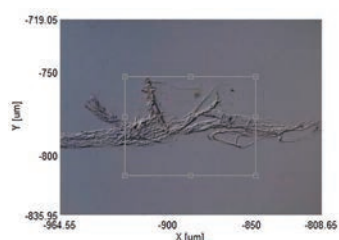
The stage is moved to a measurement point roughly by using coordinate information, and then is moved finely by using the coincidence of a recorded and current observation image (image matching technique) (Fig. 9). Since IQ Frame can move the stage to the measurement point with high position accuracy (micron-order), it is possible to measure the sample at exactly the same position/area easily and rapidly even after changing between microscopes.

### (1) Sample setting



Sets the sample.

### (2) Movement by coordinate information



Moves the stage by coordinate information which was obtained in previous measurement.

### (3) Movement by coincidence of observation image



Corrects the small displacement of measurement point by using image matching technique.

Fig. 9 Overview of image matching technique.

# Tips

## JASCO Particle Analysis

[JASCO Particle Analysis] is an add-on program for [Micro Imaging Analysis] application, and can perform particle analysis with statistical processing. It can automatically binarize observation images or chemical images, and perform various particle analyses such as determining sample size, area, perimeter, horizontal/vertical Feret diameter, aspect ratio, and circularity. Using the statistical processing function, a stacked histogram for each component, a frequency distribution table, a correlation distribution, and a component ratio can be displayed.

As examples of measurement/analysis, Raman imaging measurements of two types of rubber were performed, and the distributions of additive (calcium carbonate;  $\text{CaCO}_3$ ) in each sample were also determined. Raman imaging measurement could obtain information about the distribution of the additive, which could not be obtained from the observation view (Fig. 10).

In addition, the particle analysis of the chemical image determined the statistical distribution (such as size and circularity), and discriminated the difference between the samples.

[JASCO Particle Analysis] is effective in the statistical evaluation of particles based on the chemical information of a sample.

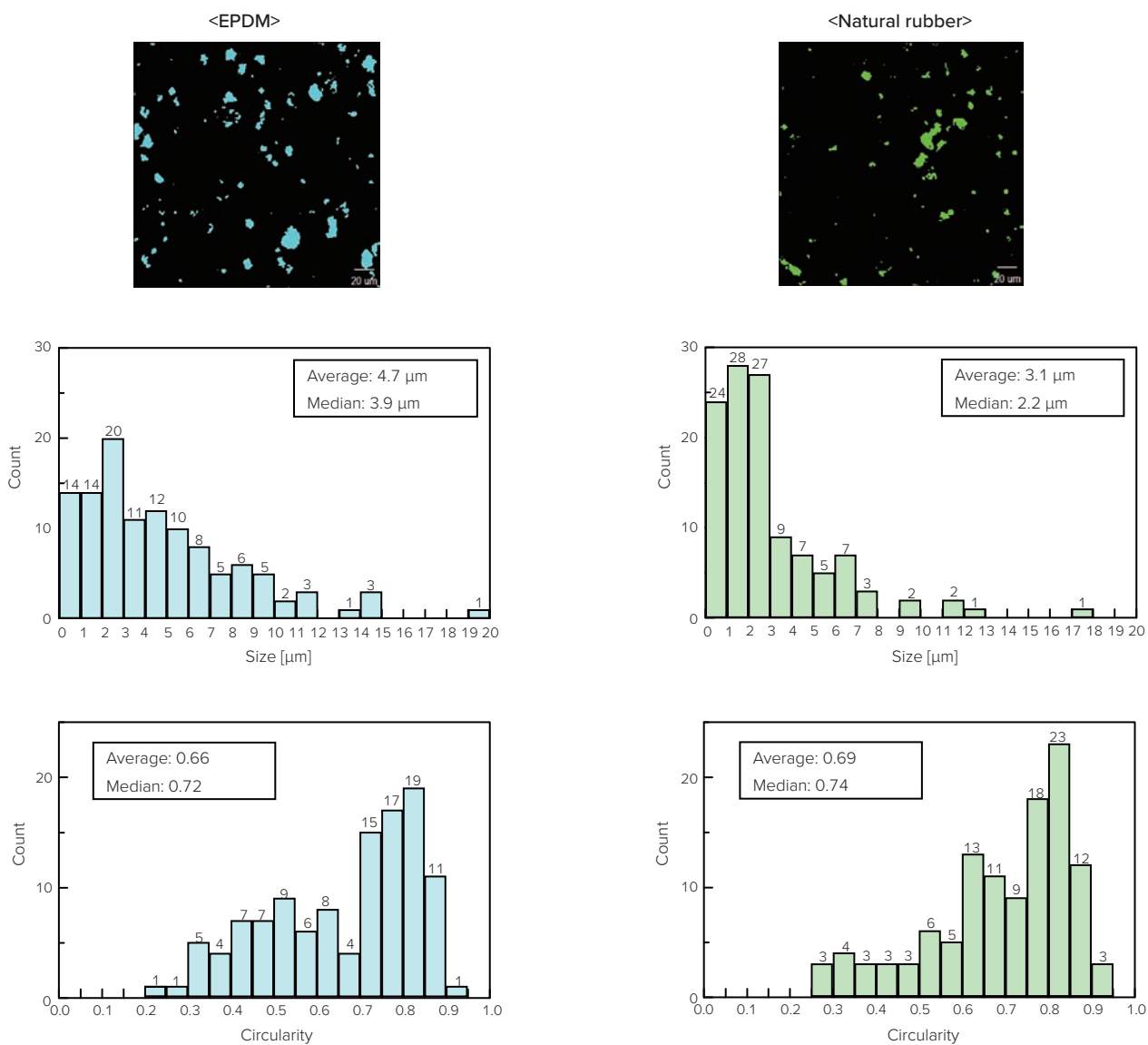


Fig. 10 Particle analysis of additive ( $\text{CaCO}_3$ ) in EPDM and natural rubber. (upper: Raman imaging measurement results of  $\text{CaCO}_3$ , middle: size histograms, lower: circularity histograms)



## Evaluating the Distribution of Components in Pharmaceutical Tablets

The distribution of active pharmaceutical ingredients (APIs) and excipients in formulated tablets affect its dissolution in the body, and it is important to evaluate this at an early stage in drug development and quality control.

Raman spectroscopy is well-known as a tool for evaluating the APIs and excipients in tablets both qualitatively and quantitatively. Since Raman imaging measurement can visualize the distribution of APIs and excipients, it is a very effective tool in pharmaceutical development and quality control.

This section shows the evaluation of component composition in a pharmaceutical tablet.

### Component Distribution in a Pharmaceutical Tablet

Raman imaging measurement was performed on a selected area of a tablet (Figs. 1, 2 and 3). Principal component spectra were calculated by multivariate curve resolution (MCR) analysis. Creating a chemical image using MCR analysis makes it possible to visualize the distribution of the APIs and excipients.

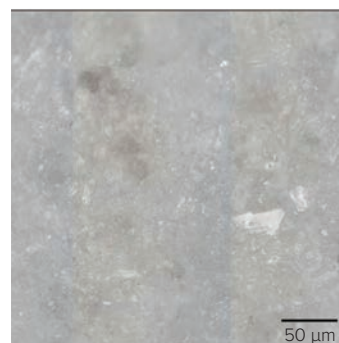


Fig. 1 Observation view.

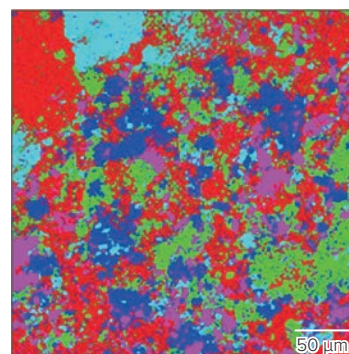


Fig. 2 Raman imaging measurement result. (pink: apronalide, aqua: caffeine, blue: lactose, red: ethenzamide, green: acetaminophen)

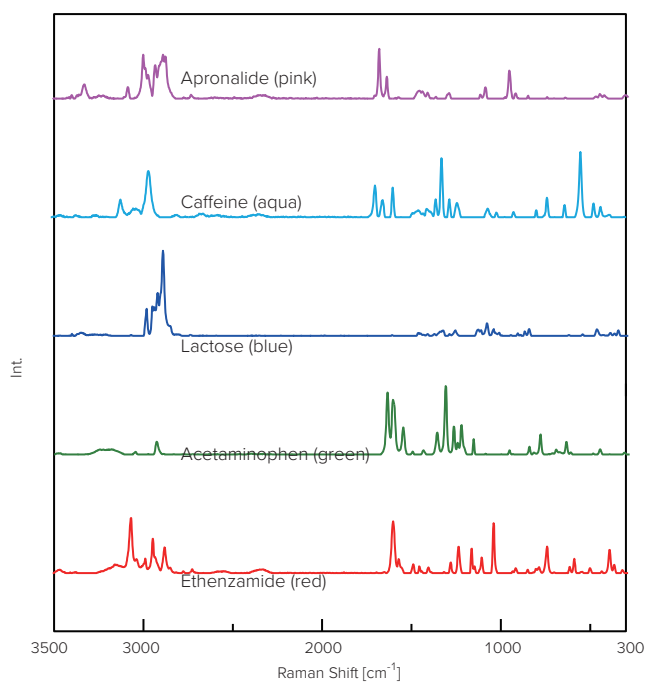
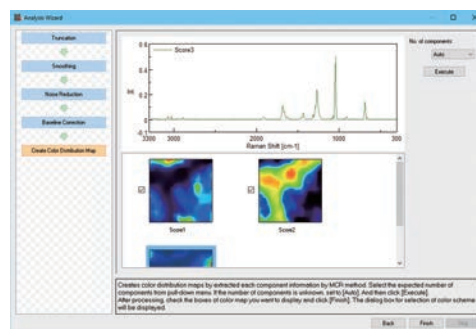


Fig. 3 Principal component spectra obtained by MCR analysis.

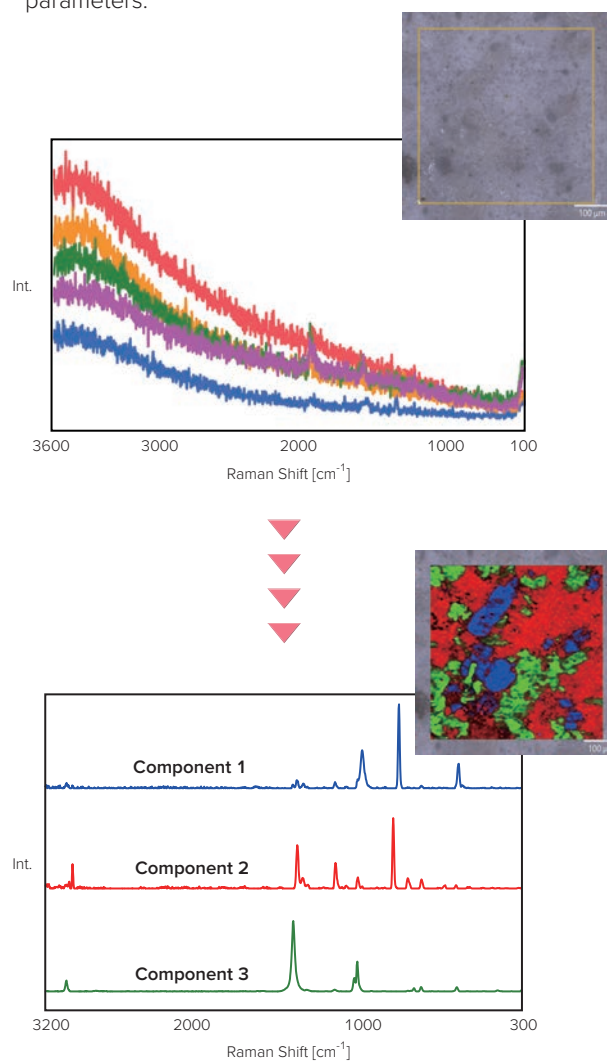
## Tips

### Analysis Wizard

The [Micro Imaging Analysis] program, can create chemical image maps of sample areas using a variety of parameters including peak height or area, half-width, correlation coefficient, multivariate analysis, etc. with a simple operation.



To simplify the process of creating color image maps, the [Analysis Wizard] guides the user with a simple to follow sequence and with guidance on how to optimize parameters.





## Evaluating the Crystal Polymorphs in Pharmaceutical Development

Crystal polymorphs are molecules that can exist with the same chemical formula but different crystal structures. Crystal structure depends on the conditions (such as temperature and pressure) used in the crystal formation process. The resulting crystal structures are conveniently classified as Forms I, II, III or  $T_a$  and  $T_b$ .

In medicine, solubility, stability and bioavailability depend on the crystal polymorphism; compounds with different crystal structures may even be misidentified as different compounds. Therefore, research into crystal polymorphism is widely used in areas such as basic studies, structure/function correlation and industrial applications including patent registration.

In the pharmaceutical industry, the study of crystal formation techniques is very important in the control of crystal structure and the manufacture of high-quality medicines. Although X-ray diffraction (XRD) and differential scanning calorimetry (DSC) are widely used in the evaluation of crystal polymorphism, they have some drawbacks. XRD cannot evaluate thermal stability, and it is difficult to measure samples with low reflectivity (less diffraction spot) such as amorphous and/or tiny crystals. Conversely, DSC can be applied to evaluate the thermal stability of a crystal, but structural information cannot be obtained.

Raman spectroscopy is becoming a commonly used analytical technique for the study of crystal polymorphism, with the following features:

- Both crystal and amorphous structures can be evaluated.
- Vibrational information of molecules can also be obtained from high wavenumber spectra.
- High spatial resolution and micro measurement can be performed.
- Sample preparation is not required.
- It is possible to monitor in-situ structural changes with temperature.

Presently, XRD is used for the basic study of crystal structure for patent registration, and Raman spectroscopy is also expected to become a more widely used technique in the pharmaceutical industry for patent registration for the above reasons.

This section introduces the evaluation of crystalline polymorphs using Raman spectroscopy.

### Measurement of Trehalose Polymorph

Raman measurements of trehalose dihydrate and trehalose anhydrate were performed (Figs. 1 and 2). It was confirmed that the peaks of molecular vibration and lattice vibration differs from each other due to differences in the crystal structure.

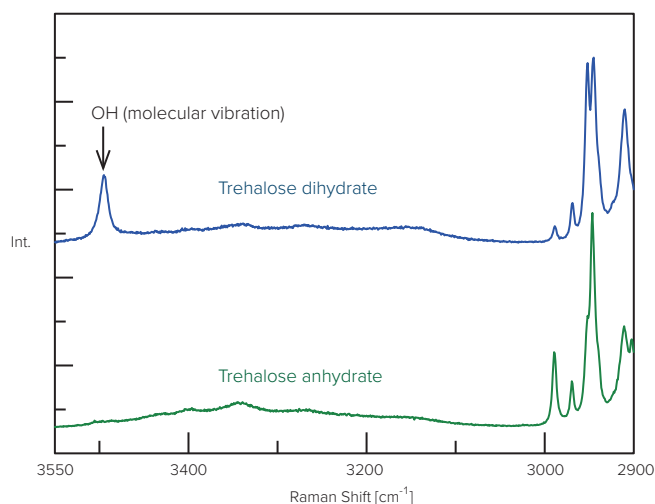


Fig. 1 Raman spectra of trehalose.

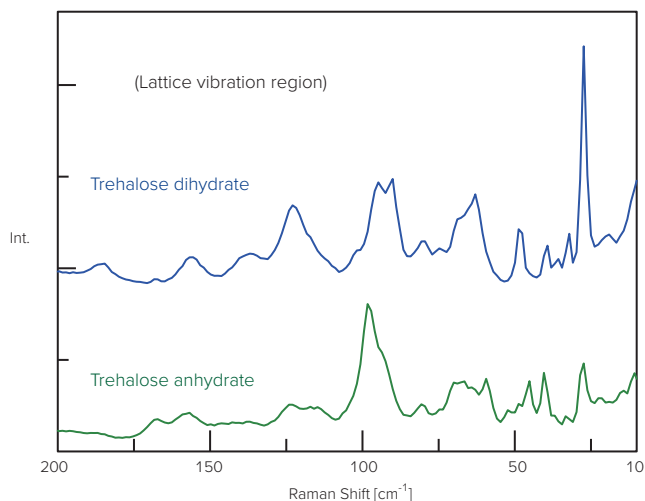


Fig. 2 Raman spectra of trehalose. (low wavenumber region)

### Measurement of Indomethacin Polymorph

Commercially available indomethacin was measured using Raman microscopy with and without a low wavenumber measurement unit (Fig. 3). It is known that indomethacin exists as three different crystal structures: alpha (acicular crystal), beta and gamma (plate crystal). Gamma is the most stable structure followed by the alpha structure. Recently, the alpha polymorph has been selectively manufactured (and patented) to be used as a topical medicine for enhanced stability and skin absorption. The method for effective manufacturing of a specified crystal structure is extremely important. Since low wavenumber measurement by Raman spectroscopy provides useful information about lattice vibration, it can be used to evaluate crystal polymorphs without any pre-treatment or damage to the sample.

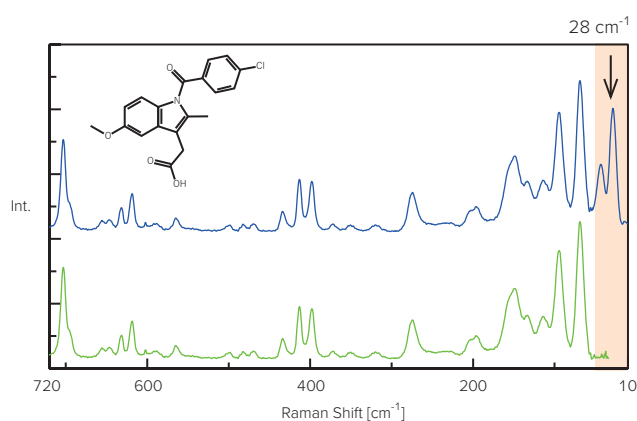


Fig. 3 Raman spectra of indomethacin. (blue: with low wavenumber measurement unit, green: without low wavenumber measurement unit)

### Measurement of Carbamazepine Polymorph

A commercially available tablet containing carbamazepine was measured using Raman microscopy (Figs. 4, 5 and 6). Since Raman spectroscopy can easily detect peaks in the wavenumber region below  $100\text{ cm}^{-1}$ , it is possible to identify differences in the crystal structure. In addition, by creating a chemical image, the distribution of the specified crystal structure can also be visualized (Figs. 5 and 6).

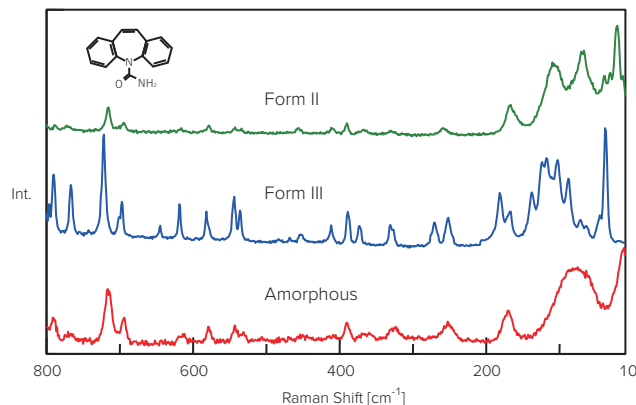


Fig. 4 Raman spectra of carbamazepine.

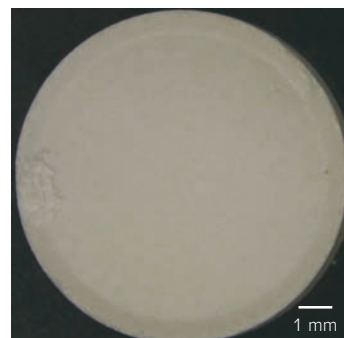


Fig. 5 Observation view of tablet.

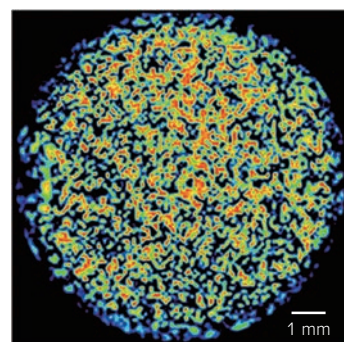


Fig. 6 Raman imaging measurement result. (Distribution of carbamazepine Form III)

## Temperature Stability Evaluation of Pharmaceutical Drugs

The stability of pharmaceutical drugs and the impact of environmental factors is important in quality control.

In this section, Raman measurement was performed on a commercially available tablet containing carbamazepine that was heated to 200 °C (Figs. 7 and 8). It was confirmed that form II was generated by heating. Raman imaging measurement could obtain the local crystal structure transition information that cannot be confirmed in the observed view.

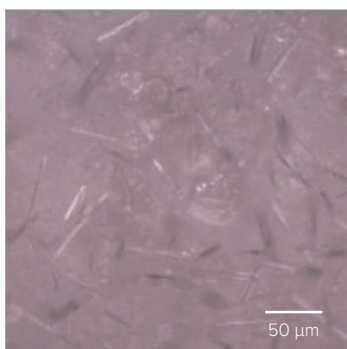


Fig. 7 Observation view (after heating).

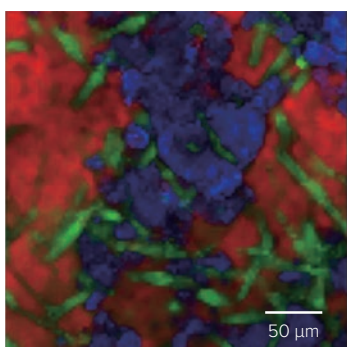


Fig. 8 Raman imaging measurement result (after heating). (red: form III, green: form II, blue: excipients, etc.)

## Tips

### Low Wavenumber Measurement

A rejection filter is necessary for excluding the Rayleigh scattering during Raman measurement. If the performance of the filter is poor, it may also exclude meaningful peaks in the low wavenumber region.

Fine angular adjustment of the rejection filter allows precise control of the exclusion of the Rayleigh scatter, improving Raman measurement in low wavenumber region (Fig. 9).



Fig. 9 Rejection filter with angle adjustment function.

Very low wavenumber measurement close to the Rayleigh scatter can be made by using up to 3 rejection filters. The incident angle of each filter can be finely adjusted (Fig. 10).



Fig. 10 Very low wavenumber measurement unit.

Adjusting the incident angle of the rejection filters finely tunes spectral acquisition, with Raman measurement in the extremely low wavenumber region (Fig. 11).

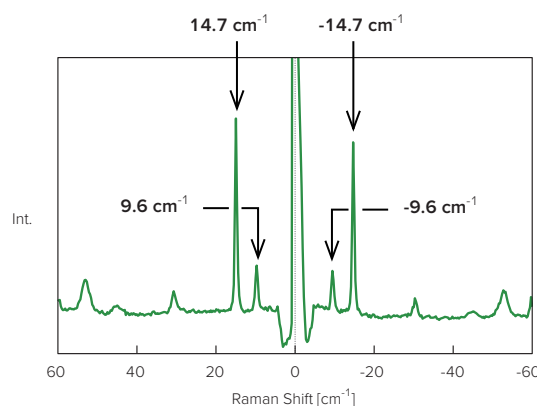


Fig. 11 Raman spectrum of L-cystine.



## Non-Destructive Analysis of Artwork and Other Cultural Assets

In the study of archaeology, art history and in the restoration of works of art, it is important to analyze and determine the materials that were historically used as pigments. Raman spectroscopy is a useful tool for non-destructive and qualitative analysis of archaeological artifacts and works of art; this is because the measurement range is wider than IR spectroscopy, which enables the measurement of not only organic pigments but also inorganic pigments that typically have absorption peaks in the low wavenumber range below  $400\text{ cm}^{-1}$ .<sup>1)</sup>

This section introduces the analysis of pigments by Raman spectroscopy.

1) Borgia, I. et al., *Journal of Cultural Heritage*, **8**, 65-68 (2007).

### Qualitative Analysis of Colorants

It is generally considered difficult to obtain good Raman spectra of colored materials because of their strong fluorescent characteristics, but it can be avoided by selecting an excitation wavelength that is not close to the absorption band in the molecule; this is because these pigments typically have strong and sharp absorption peaks in the visible region. In this experiment, water paint pigments were used as samples, which were excited using lasers with 3 different wavelengths for a comparative study.

In the case of the red pigment, a spectrum with good S/N was obtained when selecting a longer excitation wavelength (Fig. 1). For the blue pigment, good S/N was obtained with a shorter excitation wavelength (Fig. 2). And for the green pigment, a good spectrum was obtained with 633 nm excitation (Fig. 3).

When measuring the red pigment, the drift in baseline caused by fluorescence was observed even with excitation at 785 nm. Selecting 1064 nm excitation (with InGaAs detector) markedly reduced the background fluorescence (Fig. 1).

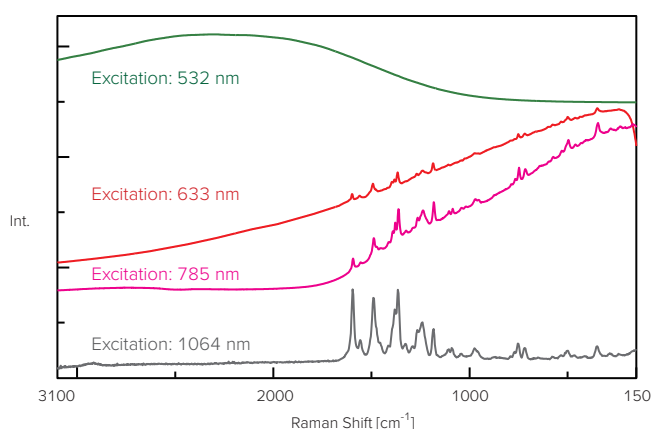


Fig. 1 Raman spectra of red pigment.

Generally, observed color is the complementary color to the absorbed light (Fig. 4). In this example, the red pigment radiates strong fluorescence when excited at 532 nm because it absorbs selectively the light in the region between green and blue. However, the green pigment that was expected to absorb red light actually shows the best S/N when excited using 633 nm in the red region. The cause of this phenomenon may be because the Raman peak of phthalocyanine, a component in the green pigment, is selectively enhanced by the red laser due to resonance Raman.

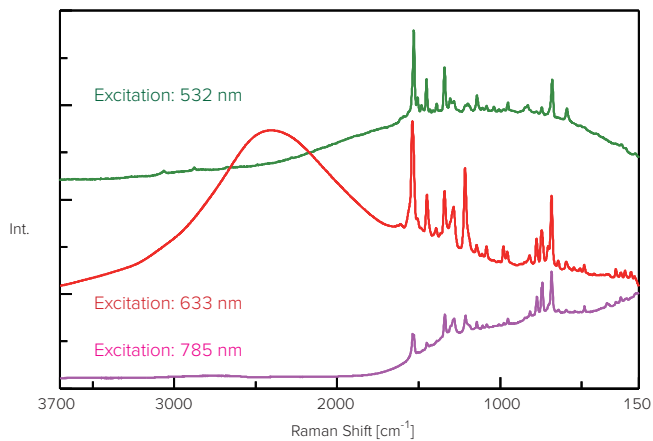


Fig. 2 Raman spectra of green pigment.

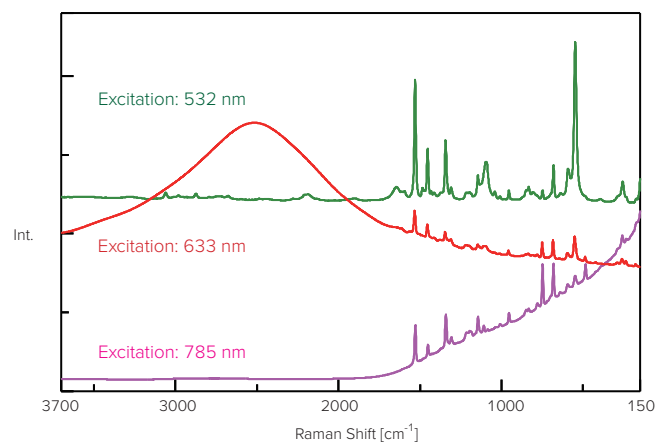


Fig. 3 Raman spectra of blue pigment.



Fig. 4 Wheel of hue.

In addition, the spectral shapes of the green and blue samples differ according to excitation wavelength; this is because the group vibration of the chromophore is caused by absorption selectively enhanced by resonance Raman.

Library search of the database does not yield any spectra match for these pigments. This is because the ratio of peak intensity is different depending on the excitation wavelength making the spectra different from the library data previously obtained from FT-Raman (1064 nm excitation). In addition, pigment components often contain various crystal polymorphs, since physical characteristics such as hue and corrosion resistance depend on the presence of different crystal polymorphs, Raman spectroscopy is proven to be a useful analytical tool to identify these.

## Combined Analysis of Toner Pigment

Combining analysis using Raman spectroscopy with other spectroscopic techniques yields complementary information. This section demonstrates examples of combined analysis using IQ Frame (refer to page 33).

As an example, a cyan toner that was set in a diamond compression cell was measured (Fig. 5).



Fig. 5 Observation view (left) and diamond cell (right).

First, the sample was measured using a UV-visible microspectrophotometer (Fig. 6), and a color calculation was performed to accurately determine the color of the toner (Fig. 7).

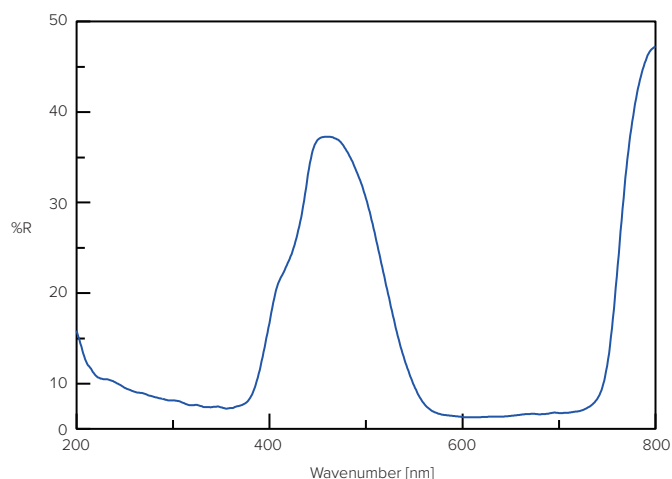


Fig. 6 Absorption spectrum of cyan toner.

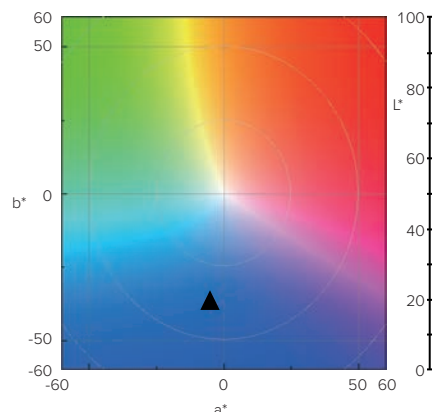


Fig. 7 Color calculation result.

Next, the sample was measured using IR microscopy, and a library search was performed using KnowItAll (Fig. 8). IR microscopy was able to identify the main component (resin) including the inside of the sample.

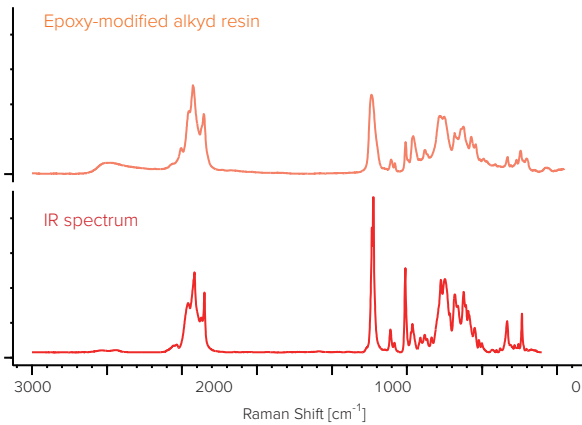


Fig. 8 IR spectrum and library search result.

Finally, the sample was measured by Raman microscopy, and a second library search was performed using KnowItAll (Fig. 9). Since the Raman measurement was performed directly in the diamond cell, it must be noted that there is a diamond peak present in the Raman spectrum. The pigment on the sample surface was identified from the Raman spectrum.

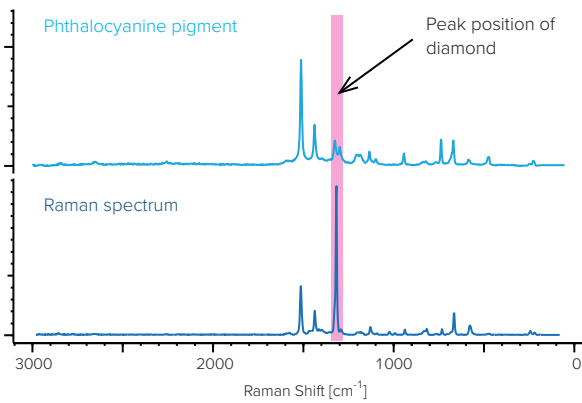


Fig. 9 Raman spectrum and library search result.

## Non-Destructive Analysis of Archaeological Art

Chemical analysis of archaeological samples is very important in the investigation of historical significance, but often artifacts cannot be moved from their location for analysis. When in-situ measurement is required for non-destructive analysis, a Raman system with a fiber probe is extremely convenient. This section shows the identification of pigments used on a wall fresco.

The sample, a wall fresco, was painted in the 16th century in a small church located in northern Italy (Fig. 10). From the Raman spectra, the components in the colored pigments (black, red, blue and white) were identified as carbon, red ochre, azurite and calcite, respectively (Fig. 11).



Fig. 10 Wall fresco.

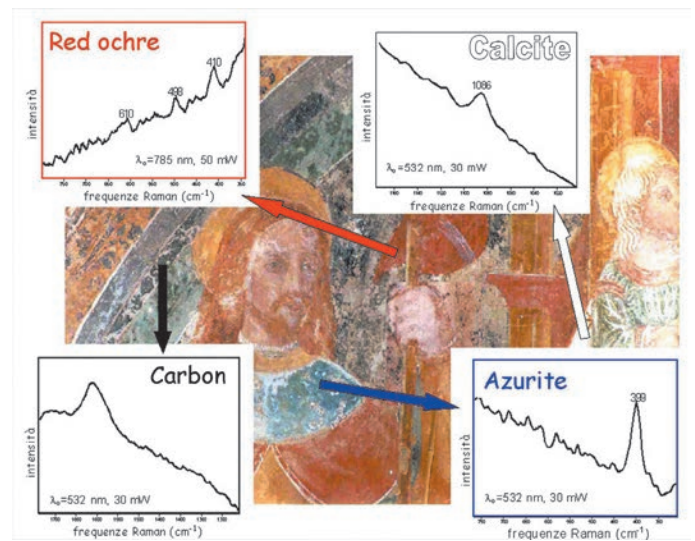


Fig. 11 Measurement result.

We would like to express our sincere gratitude to Prof. Sgamellotti of University of Perugia, Italy for providing the data.



## Forensic Analysis of Vermillion Ink

Raman spectroscopy is used to analyze molecular structure from molecular vibrations, similar to IR spectroscopy. There are several distinct advantages of Raman spectroscopy; a smaller microscopic area, spectra in the low wavenumber region can be easily acquired, the sample can be measured using a non-destructive and non-contact method, and precise information about the inside of a sample can be selectively obtained. For these reasons, Raman spectroscopy has become a key analytical technique in many applications, such as semiconductors, pharmaceuticals, and general chemistry. Recently, Raman is being more widely used in the field of criminal investigations. For example, Raman spectroscopy can be used in the examination of minute fragments of evidence and moreover, in the identification of poisonous or toxic substances and illicit drugs without opening the container.

The following points should be noted for forensic investigation. The first is interference from sample fluorescence. The most effective method to minimize fluorescence is selecting a laser wavelength that does not cause fluorescence; generally, longer wavelengths such as 785 nm or 1064 nm will result in a significant reduction in fluorescence. A second technique to reduce fluorescence is narrowing down the laser spot size or using an apertured confocal optical system, the spatial resolution in the xy-direction (and even the z-direction) can be improved, minimizing the influence of fluorescence from the matrix surrounding the point of measurement. The second issue is the potential for damage to the sample caused by laser irradiation. To avoid damage to the sample, it is important to set the optimum laser intensity by using an attenuator.

In this section we used Raman spectroscopy to analyze seal imprints. A Vermillion ink pad containing inorganic pigments such as cinnabar and other types of ink pad containing organic pigments are often used for seal imprints. These materials can be easily discriminated using Raman spectroscopy in the low wavenumber range. If the ink material can be characterized, it would be useful in improving investigative results.

### Measurement using a 532 nm Laser

Seals imprinted on three different papers were measured using a 532 nm laser (Figs. 1 and 2).

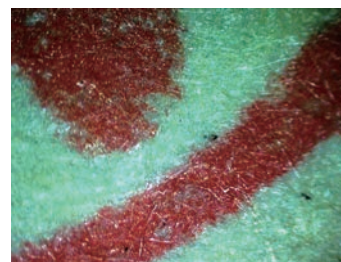


Fig. 1 Observation image of the seal.

In order to avoid damage to the sample, the laser intensity was gradually increased until optimal spectra were obtained. The fluorescence from vermilion ink or its surrounding matrix can be very strong when measured without using a confocal optical system, which makes it difficult to detect any Raman peaks. In this measurement, a confocal optical system was used and Raman measurement could be made because of the improved spatial resolution.

From the results, Raman peaks were observed in the spectrum of Seal A, though it was affected by fluorescence. In the spectrum of Seal B, some small peaks were just observable, but it was impossible to detect Raman peaks in the spectrum of Seal C.

(Raman application data: 040-AN-0009)

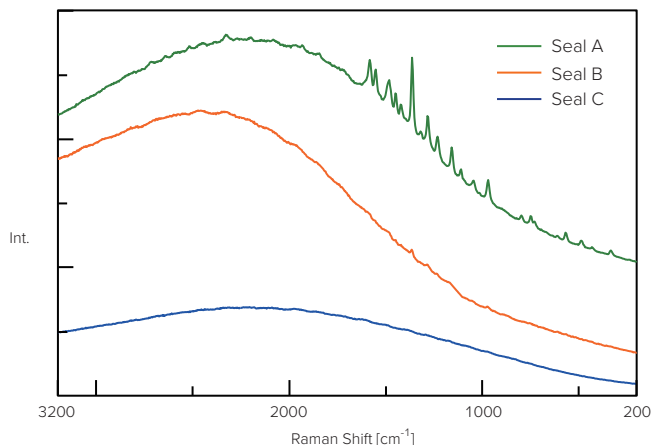


Fig. 2 Raman spectra with excitation wavelength at 532 nm.

### Measurement using a 785 nm Laser

To reduce the interference from fluorescence, Raman measurements were made using a 785 nm laser (Fig. 3). Raman peaks were observed in the spectrum of Seal A, but fluorescence was still dominant. The fluorescence was greatly reduced in the spectra of Seal B and Seal C, compared to the 532 nm laser.

When the optimum conditions are selected, such as a suitable laser wavelength, better spatial resolution and correct laser intensity, good Raman spectra can be obtained even for samples like vermilion ink that has a lot of background fluorescence.

(Raman application data: 040-AN-0009)

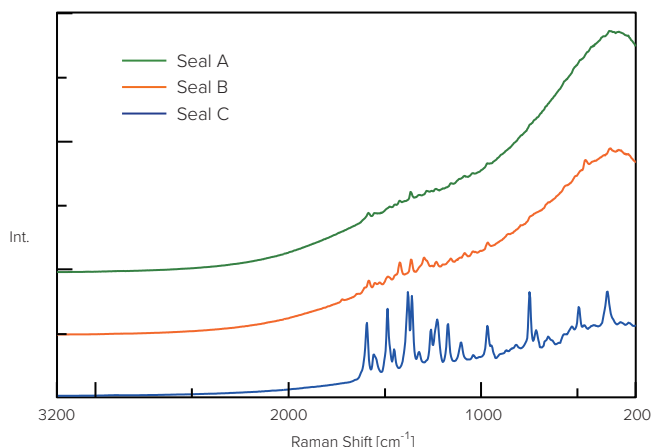


Fig. 3 Raman spectra with excitation wavelength at 785 nm.

### Analysis of the Results

Taking a closer look at the results, the three spectra (Seal A: 532 nm excitation, Seal B and C: 785 nm excitation) were processed using fluorescence correction and normalization in the analysis software (Fig. 4). The Raman spectrum (2000–600 cm⁻¹) of each sample was different and could be discriminated. Each ink sample has resin with the organic pigment. However, from the differences in the low wavenumber range (red frame) where the peaks due to inorganic substances are expected to appear, several peaks were barely seen in the spectrum of a Seal A as compared with the spectra of Seal B and Seal C. Therefore, it can be assumed that organic pigments are used primarily in ink of Seal A, while Seal B and Seal C contain inorganic pigment in the resin of the vermilion ink pad. If a library of reference spectral for different types of vermilion ink pad and other inks was available, imprints can be analyzed and identified by comparing the obtained spectra of imprint with this reference data.

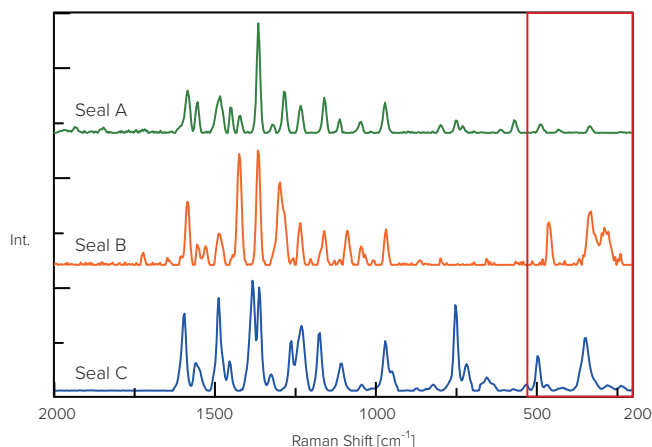
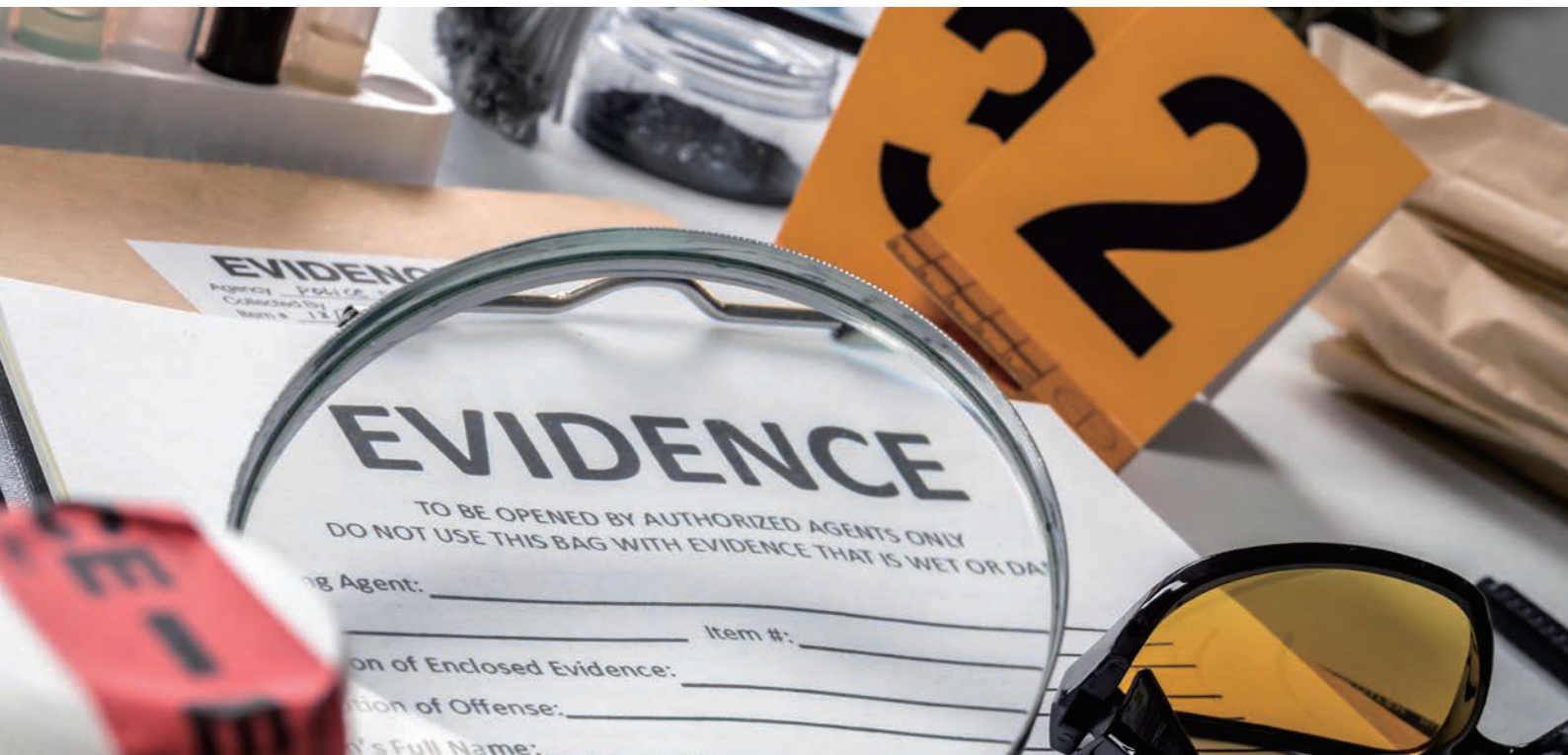


Fig. 4 Spectra after fluorescence correction (normalized view).

As mentioned above, in Raman spectroscopy measurement is made using a non-contact method with very simple operation; this makes it a powerful tool when the sample is limited and non-destructive testing is required.

(Raman application data: 040-AN-0009)



## Commercial Pen Ink Identification in a Handwriting Document

In Raman spectroscopy, spatial resolution is a key factor in obtaining well discriminated data without mixing information from other components. Since the performance of a confocal optical system affects the spatial resolution, achieving good data depends on the instrument design and quality of the optical system.

To demonstrate what can be achieved using Raman measurement, this section shows the analysis of six types of commercial pen ink in a handwritten document.

### Raman Spectra of Each Pen

Six different types of commercial pen ink used in handwritten documents were measured to verify the possibility of identification (Figs. 1, 2 and 3).



Fig. 1 Six types of commercial pen (left) and their ink on handwritten document (right).

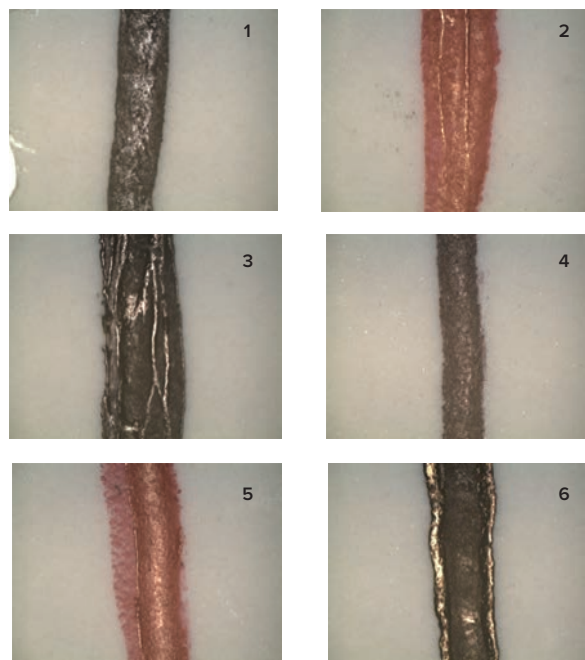


Fig. 2 Observation view.

Sample #2 was measured with a 785 nm excitation because the influence of fluorescence was too strong with 532nm excitation.

In the measurement of all samples, Raman spectra could be obtained without the influence of the paper (cellulose). Raman spectra of sample #3 could not be obtained because the influence of fluorescence was too strong even at 785 nm excitation.

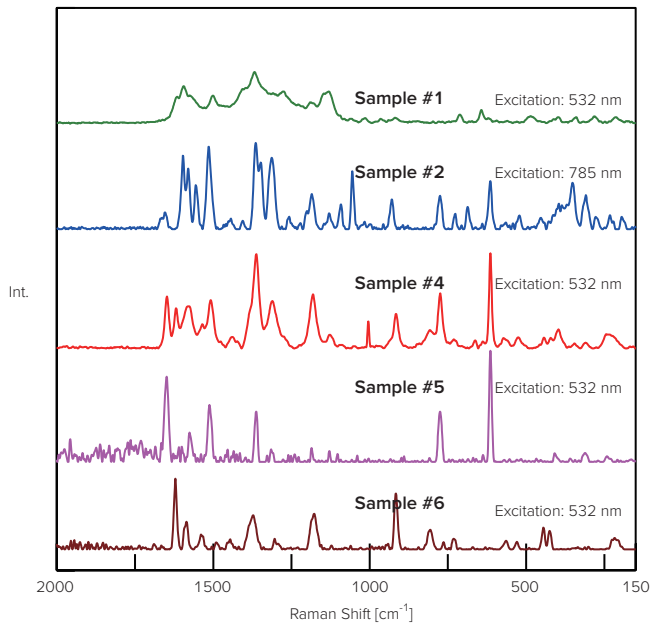


Fig. 3 Obtained Raman spectra.  
(After fluorescence correction, Y-axis offset)

Ink components of the vertical lines (second stroke) were detected at each intersection, and it means that Raman spectroscopy could selectively detect the surface information.

The results indicate that Raman spectroscopy is a useful tool to determine the order of a handwriting intersection.

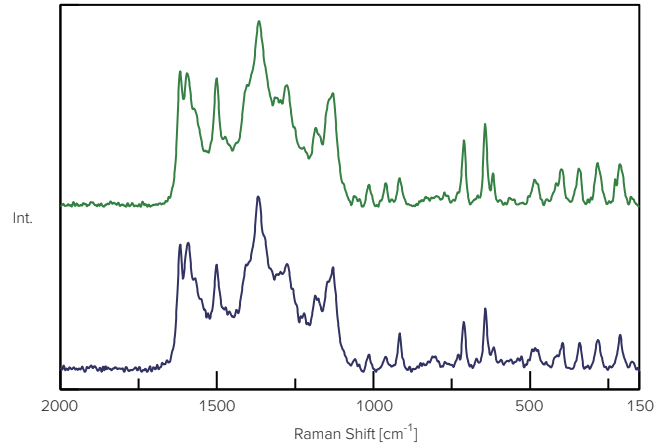


Fig. 5 Raman spectra of intersections.  
green: black pen #1 (vertical line) and black pen #4 (horizontal line)  
blue: black pen #1 (vertical line) and black pen #6 (horizontal line)

After registering reference data of each product in KnowItAll, a library search can be made to identify unknown pen ink samples.

### Determining the Stroke Order of Intersections using Raman Spectroscopy

Using three different black pens (#1, #4 and #6), vertical lines were drawn after drawing horizontal lines (Fig. 4), and the six intersections were measured to see if the stroke order could be determined (Figs. 5, 6 and 7).

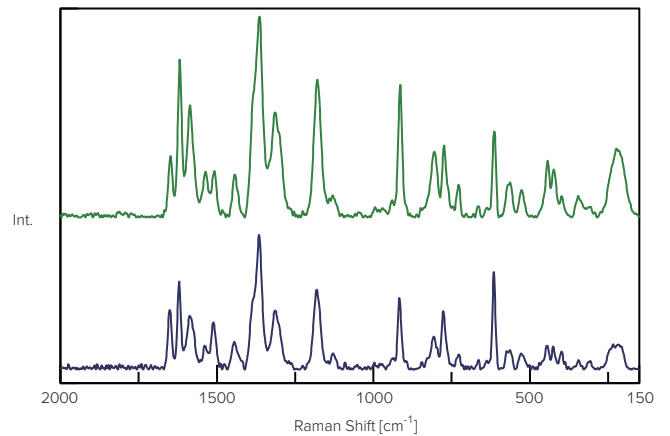


Fig. 6 Raman spectra of intersections.  
green: black pen #4 (vertical line) and black pen #1 (horizontal line)  
blue: black pen #4 (vertical line) and black pen #6 (horizontal line)

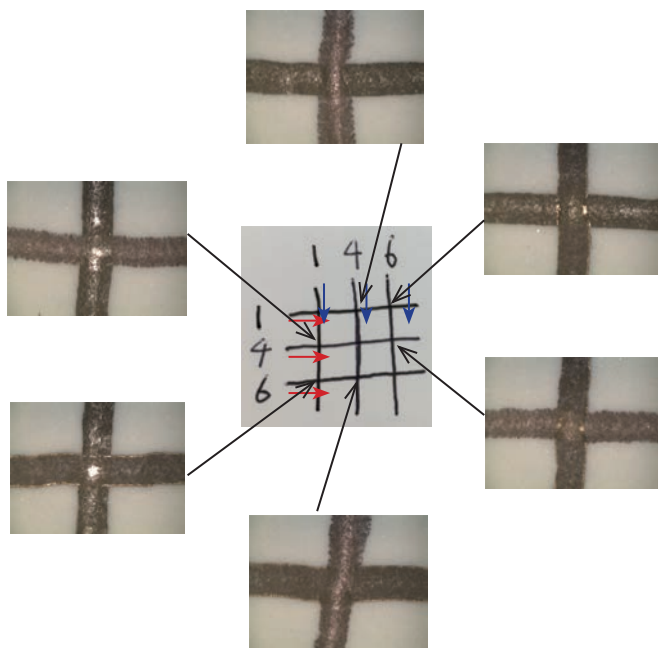


Fig. 4 Observation view of intersection.  
(red arrow: first stroke, blue arrow: second stroke)

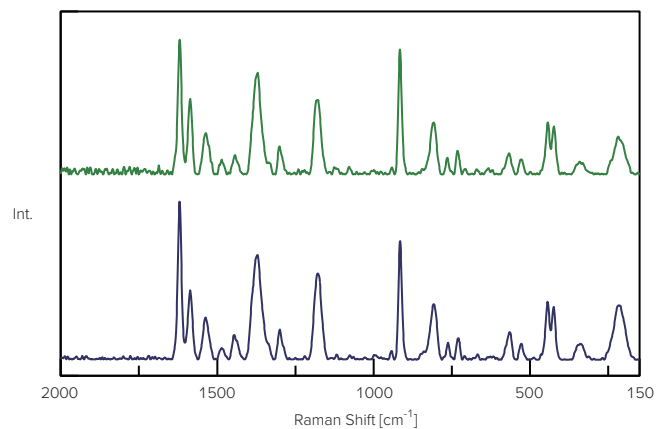


Fig. 7 Raman spectra of intersections.  
green: black pen #6 (vertical line) and black pen #1 (horizontal line)  
blue: black pen #6 (vertical line) and black pen #4 (horizontal line)

## Tips

### Spectral Search Program - KnowItAll™

WILEY's KnowItAll, which is a highly regarded data search software, is used as standard. The search software starts up with one click from the analysis program (Fig. 8).

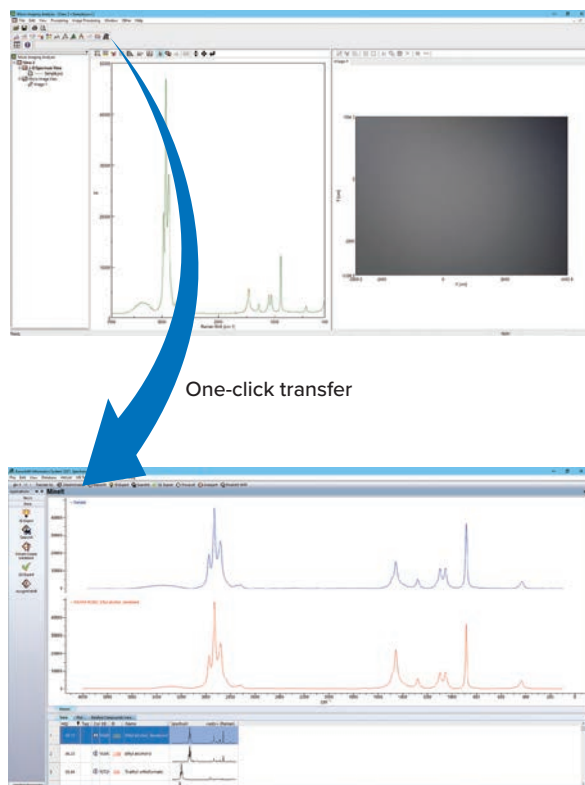


Fig. 8 KnowItAll.

KnowItAll includes various functions such as spectral/peak/structure search, mixture analysis, spectral interpretation support and more. In addition, 645 organic compound spectra and 650 JASCO original spectra are installed as standard as a reference library. WILEY's 25,000 Raman spectra are also available as an option.

#### Mixture analysis

For unknown samples containing multiple components, up to five components can be identified from one spectrum.

#### Spectral interpretation support (Analyzelt™ Raman)

This function can find the functional groups that match the peaks of spectrum.

#### User database builder

Creating a user-defined database, it can register the sample spectra, structural formula and physical properties. It enables to unitarily manage and share the measurement data.

#### Multi-technique simultaneous spectral searching

KnowItAll's multi-technique simultaneous spectral searching allows to search the IR and Raman spectra simultaneously and find the most relevant hits in each database linked to each other by chemical structure.



**JASCO INTERNATIONAL CO., LTD.**

11-10, Myojin-cho 1-chome, Hachioji, Tokyo 192-0046, Japan

Tel: +81-42-649-3247 Fax: +81-42-649-3518 <http://www.jascoint.co.jp/english/>

Australia, Hong Kong, India, Indonesia, Korea, Malaysia, New Zealand,

Pakistan, Philippines, Russia, Singapore, Taiwan, Thailand, Vietnam

**JASCO INCORPORATED**

28600 Mary's Court, Easton, Maryland 21601, U.S.A.

Tel: +1-410-822-1220 Fax: +1-410-822-7526 Web: [www.jascoinc.com](http://www.jascoinc.com)

Argentina, Bolivia, Brazil, Canada, Chile, Colombia, Costa Rica, Guatemala, Mexico,

Paraguay, Peru, Puerto Rico, United States of America, Uruguay, Venezuela

**JASCO EUROPE S.R.L.**

Via Luigi Cadorna 1, 23894 Cremella (LC), Italy

Tel: +39-039-9215811 Fax: +39-039-9215835 Web: [www.jascoeurope.com](http://www.jascoeurope.com)

**JASCO Deutschland** [www.jasco.de](http://www.jasco.de) | **JASCO UK** [www.jasco.co.uk](http://www.jasco.co.uk) | **JASCO France** [www.jasco.fr](http://www.jasco.fr)

**JASCO Benelux** [www.jasco.nl](http://www.jasco.nl) | **JASCO Spain** [www.jasco-spain.com](http://www.jasco-spain.com)

Algeria, Austria, Belgium, Cyprus, Denmark, Egypt, Finland, France, Germany, Greece, Hungary, Iran, Iraq, Israel, Italy, Jordan, Kuwait, Lebanon, Luxembourg, Morocco, Netherlands, Norway, Poland, Portugal, Romania, Saudi

Arabia, South Africa, Spain, Sweden Switzerland, Tunisia, Turkey, United Arab Emirates, United Kingdom, Yemen

**JASCO China (Shanghai) Co., Ltd.**

Room No.D, 10F, World Plaza, 855 Pudong South Road, Pudong New Area, chi

Tel: +86-21-6888-7871 Fax: +86-21-6888-7879 <http://www.jasco-global.com>



Products described herein are  
designed and manufactured by  
ISO-9001- and ISO-14001-certified  
JASCO Corporation